
TSI-Bench: Benchmarking Time Series Imputation

Wenjie Du^{1,*†}, Jun Wang^{1,2,*}, Linglong Qian^{1,3,*}, Yiyuan Yang^{1,4,*}, Fanxing Liu⁵, Zepu Wang⁶
 Zina Ibrahim³, Haoxin Liu⁷, Zhiyuan Zhao⁷, Yingjie Zhou^{5†}, Wenjia Wang⁹
 Kaize Ding⁸, Yuxuan Liang⁹, B. Aditya Prakash⁷, Qingsong Wen^{10†}

¹PyPOTS Research, ²HKUST, ³King’s College London, ⁴University of Oxford, ⁵Sichuan University
⁶University of Washington, ⁷GaTech, ⁸Northwest University, ⁹HKUST(GZ), ¹⁰Squirrel AI

Abstract

Effective imputation is a crucial preprocessing step for time series analysis. Despite the development of numerous deep learning algorithms for time series imputation, the community lacks standardized and comprehensive benchmark platforms to effectively evaluate imputation performance across different settings. Moreover, although many deep learning forecasting algorithms have demonstrated excellent performance, whether their modeling achievements can be transferred to time series imputation tasks remains unexplored. To bridge these gaps, we develop TSI-Bench, the first (to our knowledge) comprehensive benchmark suite for time series imputation utilizing deep learning techniques. The TSI-Bench pipeline standardizes experimental settings to enable fair evaluation of imputation algorithms and identification of meaningful insights into the influence of domain-appropriate missingness ratios and patterns on model performance. Furthermore, TSI-Bench innovatively provides a systematic paradigm to tailor time series forecasting algorithms for imputation purposes. Our extensive study across 34,804 experiments, 28 algorithms, and 8 datasets with diverse missingness scenarios demonstrates TSI-Bench’s effectiveness in diverse downstream tasks and potential to unlock future directions in time series imputation research and analysis. The source code and experiment logs are available at https://github.com/WenjieDu/Awesome_Imputation.

1 Introduction

Time series data is widely used in many application domains [1, 2, 3, 4], such as air quality monitoring [5], energy systems [6], traffic [7], and healthcare [8]. However, due to sensor malfunctions, environmental interference, privacy considerations, and other factors, the time series data available for analysis may be incomplete. The absence of complete data can greatly undermine a model’s ability to accurately capture the domain for downstream tasks. By imputing missing values in time series data, the underlying mechanisms leading to missingness can be restored, thereby improving the data completeness and reliability for subsequent analysis and model construction.

The current research landscape in time series imputation is marked by inconsistencies, knowledge gaps, and wide performance disparities reported in literature reviews [9, 10]. These variations arise from differences in data characteristics and dimensionalities, domain-specific missingness patterns, and task-specific requirements. They are further amplified by the heterogeneity of implementation, experiment designs, and evaluation settings. This complicates model and study comparisons, significantly influencing algorithm performance, but remains deeply under-explored [11].

*Equal contribution; †Corresponding authors.

To bridge existing gaps, we design (to our best knowledge) the first comprehensive time series imputation benchmark, named TSI-Bench. Built on top of an *in-house developed imputation suite* encompassing 28 highly-performing time-series imputation and forecasting algorithms, TSI-Bench enables efficiently and fairly evaluating newly proposed methods against existing baselines via a standardized *ecosystem* with a wide range of data preprocessing, missingness simulation and performance evaluation techniques ready for use by researchers to tailor the imputation task according to the needs presented by their datasets, application domains and downstream tasks. Notably, due to forecasting being intertwined with imputation, TSI-Bench also incorporates a systematic paradigm to leverage time series forecasting models for imputation purposes.

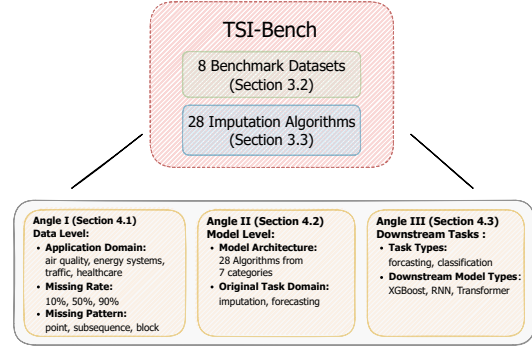


Figure 1: An overview of TSI-Bench.

The primary contributions of TSI-Bench are as follows:

- **The first comprehensive benchmark for evaluating time series imputation tasks**, encompassing **28** ready-to-use algorithms spanning both prediction-based and imputation-based approaches. The benchmark provides eight datasets across four diverse domains (air quality, traffic, electricity, and healthcare) and varying in dimensionality, missingness patterns, and data types.
- **TSI-Bench provides research and application-driven benchmarking perspectives**, enabling standardized analysis of the four critical angles of the imputation process we have identified by studying the requirements of various domains: i). the ability to simulate different degrees of missingness and analyze the effect on model performance; ii). the ability to incorporate variations of missingness patterns (e.g., subsequence missing and block missing) in time series according to domain-specific requirements, in addition to single-point missingness in a time series; iii). the types of imputation or forecasting models employed; iv). the expected downstream tasks. Any researcher encountered missing data can use TSI-Bench to explore the suitability of different imputation paradigms to one’s specific problem, dataset, and downstream task.
- **Identification and addressing of limitations inherent in the existing evaluation schemes for TSI to ensure rigorous and equitable comparisons.** We build an open-source ecosystem that encompasses a standardized pipeline for data preprocessing, flexible and user-driven missingness simulation, metric utilization, and hyper-parameter tuning. This ecosystem not only facilitates effortless reproduction of our results but also provides users with the tools to assess and integrate their datasets and models into our ecosystem with ease.

Our collective experimental efforts with TSI-Bench assess the efficacy of the different algorithms in a total of **34,804 experiments**. Our extensive experiments reveal the following **key findings**: (1) Different missing patterns and rates significantly influence the performance of imputation methods and none of the 28 algorithms significantly outperforms the others across all settings, emphasizing the importance of the model tuning and data processing capabilities enabled by TSI-Bench ; (2) Forecasting architectures demonstrate effectiveness when used as an imputation backbone; (3) When coupled with domain-informed data processing and simulation of missingness patterns, imputation significantly enhances the data quality and thus boosts downstream task performance.

2 Preliminaries and Related Work

Problem Definition A time series sequence of length L can be represented by a matrix $\mathbf{X} = (\mathbf{x}_1, \mathbf{x}_2, \dots, \mathbf{x}_L)^\top \in \mathbf{R}^{D \times L}$, with D being the data dimension. An observation $\mathbf{x}_t \in \mathbf{R}^{1 \times D}$ is acquired at some timestep t . In scenarios involving missing data, each multivariate time series consists of an observed and missing component, i.e., $\mathbf{X} = \{\mathbf{X}^o, \mathbf{X}^m\}$. To encode missingness, we introduce a mask matrix $\mathbf{M} \in \mathbf{R}^{D \times L}$ to represent the existence components of \mathbf{X}^o , i.e., $M_{d,l} = 1$ if $\mathbf{X}_{d,l}^o$ exists, otherwise $M_{d,l} = 0$. We subsequently define the imputation task as follows.

Definition 1 (Time Series Imputation) Given a reconstructed time series $\bar{\mathbf{X}}$ by an imputer, the objective of time series imputation is to obtain an imputed time series,

$$\hat{\mathbf{X}} = \mathbf{M} \odot \mathbf{X}^o + (1 - \mathbf{M}) \odot \bar{\mathbf{X}}, \quad (1)$$

so as to (i) minimize the discrepancy between the imputed time series $\hat{\mathbf{X}}$ and the real complete time series \mathbf{X} as possible, or (ii) improve the efficacy of downstream tasks when using $\hat{\mathbf{X}}$ compared to using \mathbf{X}^o only. \odot denotes the element-wise multiplication.

Related Work - Imputation Methods Deep imputation methods have recently gained popularity in handling missing values in time series data due to their ability to model the nonlinearities and temporal patterns inherent in time series. The literature contains a wide range of deep imputation methods, which can be broadly classified as either predictive or generative.

Predictive imputation methods aim to consistently predict deterministic values for missing components within the time series [12, 13, 14, 15, 16, 17]. Existing models employ a variety of neural network architectures, including Recurrent Neural Networks (RNNs), Convolutional Neural Networks (CNNs), Graph Neural Network (GNN), and attention mechanisms. Highly cited examples include GRU-D [18] and BRITS [19], which achieve improved imputation performance by integrating a time-decay mechanism into RNNs to capture irregularities caused by missing values. TimesNet [13] is a highly-performing CNN model that incorporates a Fast Fourier Transformation to restructure 1D time series into a 2D format. Finally, SAITS [20] is an attention-based model comprising two diagonal-masked self-attention blocks and a weighted-combination block, which leverages attention weights and missingness indicators to enhance imputation precision.

Generative deep imputation models, built upon generative models such as VAEs, GANs, and diffusion models, are distinguished by their ability to generate varied outputs for missing observations, reflecting the inherent uncertainty of the imputation process [21, 22, 23, 24, 25, 26, 27]. Examples include GP-VAE [28], which exploits a Gaussian process as a prior distribution to model temporal dependencies in the incomplete time series; US-GAN [29] increases the complexity of discriminator training by compromising the masking matrix, subsequently leading to the improvement of generator performance through adversarial dynamics; and finally CSDI [30] adapts diffusion models for TSI through a conditioned training strategy by employing a subset of the observed data as conditional inputs to guide the generation process of the missing segments within the time series.

Related Work - Forecasting Frameworks for Imputation In recent years, numerous deep learning architectures have exhibited exceptional performance in time series forecasting problems. These include Transformer-based structures [31, 32, 33], graph-based structures [34, 35, 36, 37], and MLP-based structures [38, 39, 40].

Transformers excel at time series forecasting due to their ability to model long-range dependencies and capture complex temporal patterns [41]. Examples include Informer [42] and Crossformer [43], which utilize different attention mechanisms to weigh the importance of different time steps dynamically. This is particularly beneficial for time series data, which often contains long-term dependencies and intricate patterns. At the same time, researchers showed that simple linear models can sometimes outperform Transformer architectures in long-term time series forecasting tasks [44]. MLP structures, known for their lower complexity and computational efficiency, have attracted growing interest from researchers. For instance, TSMixer [39] extends the MLP mixer concept from computer vision [45] to time series forecasting by performing mixing operations along both time and feature dimensions [38]. Other innovative MLP-based designs, such as Koopa [46] and FITS [47], further highlight the promising potential of MLP approaches in advancing time series forecasting.

The progress in forecasting models has the potential to be beneficial in imputation problems. Theoretically, forecasting and imputation problems can be regarded as two similar tasks in time series analysis, as both require obtaining temporal representations of existing time series data to predict future values [48] or to impute missing values [10, 49]. Given that time series forecasting is a highly active research area within time series analysis, a framework that enables researchers to directly apply forecasting methods to imputation challenges could potentially lead to the development of more efficient imputation techniques. This, in turn, might further advance research in time series analysis.

3 The Setup of TSI-Bench

In this section, we introduce the models that we evaluate in the experiments, information of datasets, and relevant implementation details.

3.1 TSI-Bench Suite

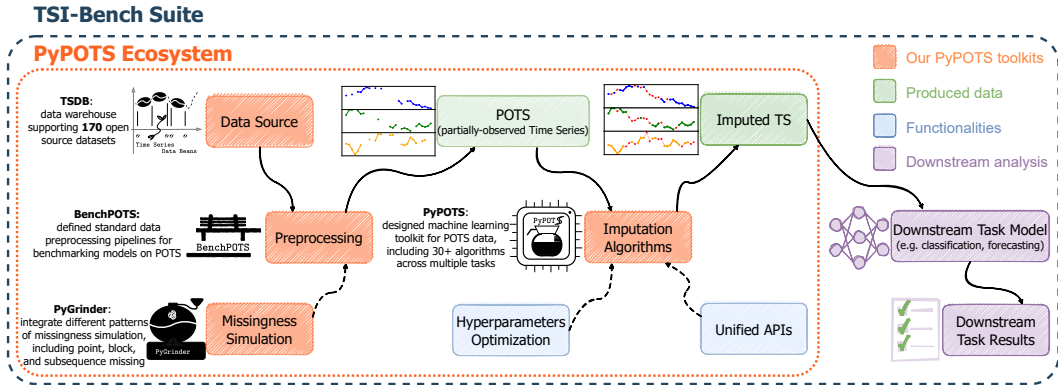


Figure 2: Overview of the designed TSI-Bench suite.

TSI-Bench is a standardized suite that streamlines the imputation process and downstream tasks and is based on our PyPOTS Ecosystem [50]. PyPOTS is a toolkit providing easy standardized access to imputation, classification, clustering, and forecasting algorithms and is openly available on GitHub: <https://github.com/WenjieDu/PyPOTS>. PyPOTS covers the entire imputation workflow from data loading, data processing, and model building, to data imputation. Our TSI-Bench workflow is shown in Figure 2. First, data is loaded from our time series database, TSDB, which serves as the data warehouse. The loaded data is then transformed into partially-observed time series (POTS) using PyGrinder, which performs flexible and user-driven missingness simulation. Next, the POTS is processed with BenchPOTS, which provides standard data preprocessing pipelines to benchmark machine learning algorithms on POTS. Subsequently, the preprocessed time series is input into an imputation model implemented in PyPOTS to estimate the missing values, resulting in imputed time series. Finally, the imputed data is offered to downstream models to perform additional data analysis tasks, e.g. classification, regression, and forecasting.

3.2 Datasets

In TSI-Bench, we select **8** diverse and representative datasets from four domains for experiments, across **air quality**, **traffic**, **electricity**, and **healthcare**. In **air quality** domain, the **BeijingAir** dataset includes hourly data on six pollutants and meteorological variables from 12 Beijing sites [51]. The **ItalyAir** dataset contains 9358 hourly records of chemical sensor responses and pollutant concentrations from March 2004 to February 2005 [52]. In **traffic**, the **PeMS** dataset provides hourly road occupancy rates from San Francisco Bay area freeways. The **Pedestrian** dataset features automated pedestrian counts in Melbourne for 2017 [53]. In **electricity**, the Electricity dataset records hourly consumption for 370 clients, while the ETT dataset includes power load and oil temperature data, using the **ETTh1** subset [32]. For **healthcare**, the **PhysioNet2012** dataset has 12,000 ICU patient records focusing on predicting in-hospital mortality, despite 80% missing values [54], and the **PhysioNet2019** dataset includes clinical data from 40,336 ICU patients, using subset A [55].

3.3 Models

To comprehensively evaluate the effectiveness of various models in the time series imputation task, we employ **28** different models already incorporated into the PyPOTS Ecosystem, each based on distinct architectures and focusing on different original tasks. These models include **Transformer architectures** like Transformer [56], Pyraformer [57], Autoformer [31], Informer [42], Crossformer [43], PatchTST [33], ETSformer [58], Nonstationary (short for Nonstationary Transformer) [59], SAITS [20], and iTransformer [60]; **RNN architectures** such as MRNN [61], BRITS [19], and GRUD [62]; **CNN architectures** including MICN [63], SCINet [64] and TimesNet [13]; **GNN architectures** like StemGNN [34]; **MLP architectures** like FiLM [65], DLinear [44], Koopa [66] and FreTS [67]; **Generative architectures** based on VAE, GAN, and diffusion models such as GP-VAE [28], US-GAN [68], and CSDI [30]. Besides, we also applied some **Traditional methods** such as Mean, Median, LOCF (Last Observation Carried Forward), and Linear interpolation. For the original forecasting backbones (Transformer, Pyraformer, Autoformer, etc.), the embedding

Table 1: Imputation performance with 10% point missingness, shown as MAE (standard deviation). For each dataset, the best performance is indicated by bold black text, the second-best performance by normal black text, and the third-best performance by bold dark gray.

	BeijingAir	ItalyAir	PeMS	Pedestrian	ETT_h1	Electricity	PhysioNet2012	PhysioNet2019
iTransformer	0.123 (0.005)	0.223 (0.014)	0.226 (0.001)	0.148 (0.005)	0.263 (0.004)	0.571 (0.178)	0.379 (0.002)	0.462 (0.006)
SAITS	0.155 (0.004)	0.185 (0.010)	0.287 (0.001)	0.131 (0.006)	0.144 (0.006)	1.377 (0.026)	0.257 (0.019)	0.352 (0.005)
Nonstationary	0.209 (0.002)	0.266 (0.007)	0.331 (0.017)	0.453 (0.024)	0.359 (0.013)	0.213 (0.014)	0.410 (0.002)	0.458 (0.001)
ETSformer	0.187 (0.002)	0.259 (0.004)	0.347 (0.006)	0.207 (0.011)	0.227 (0.007)	0.412 (0.005)	0.373 (0.003)	0.451 (0.005)
PatchTST	0.198 (0.011)	0.274 (0.026)	0.330 (0.013)	0.126 (0.003)	0.240 (0.013)	0.550 (0.039)	0.301 (0.011)	0.420 (0.007)
Crossformer	0.184 (0.004)	0.246 (0.011)	0.337 (0.007)	0.119 (0.005)	0.232 (0.008)	0.540 (0.034)	0.525 (0.202)	0.378 (0.007)
Informer	0.148 (0.002)	0.205 (0.008)	0.302 (0.003)	0.154 (0.010)	0.167 (0.006)	1.291 (0.031)	0.297 (0.003)	0.403 (0.002)
Autoformer	0.257 (0.012)	0.295 (0.008)	0.598 (0.074)	0.197 (0.008)	0.267 (0.008)	0.748 (0.027)	0.417 (0.009)	0.476 (0.002)
Pyraformer	0.178 (0.004)	0.217 (0.006)	0.285 (0.003)	0.153 (0.012)	0.182 (0.008)	1.096 (0.033)	0.294 (0.002)	0.387 (0.004)
Transformer	0.142 (0.001)	0.191 (0.010)	0.294 (0.002)	0.136 (0.009)	0.178 (0.015)	1.316 (0.036)	0.259 (0.006)	0.341 (0.002)
BRITS	0.127 (0.001)	0.235 (0.007)	0.271 (0.000)	0.149 (0.005)	0.145 (0.002)	0.971 (0.016)	0.297 (0.001)	0.355 (0.001)
MRNN	0.568 (0.002)	0.638 (0.003)	0.624 (0.000)	0.735 (0.001)	0.789 (0.019)	1.824 (0.005)	0.708 (0.029)	0.778 (0.015)
GRU4Rec	0.233 (0.002)	0.368 (0.012)	0.355 (0.002)	0.204 (0.008)	0.325 (0.004)	0.976 (0.015)	0.450 (0.004)	0.471 (0.001)
TimesNet	0.230 (0.010)	0.280 (0.004)	0.312 (0.001)	0.157 (0.008)	0.254 (0.008)	1.011 (0.016)	0.353 (0.003)	0.394 (0.003)
MICN	0.203 (0.001)	0.283 (0.004)	0.281 (0.003)	/	0.267 (0.010)	0.392 (0.006)	0.378 (0.013)	0.461 (0.007)
SCINet	0.191 (0.011)	0.288 (0.010)	0.487 (0.101)	0.149 (0.012)	0.246 (0.019)	0.581 (0.015)	0.341 (0.005)	0.427 (0.002)
StemGNN	0.161 (0.002)	0.260 (0.008)	0.493 (0.079)	0.127 (0.006)	0.248 (0.012)	1.360 (0.078)	0.331 (0.001)	0.416 (0.002)
FrETS	0.211 (0.008)	0.273 (0.008)	0.396 (0.027)	0.138 (0.004)	0.262 (0.029)	0.718 (0.043)	0.315 (0.008)	0.406 (0.017)
Koopa	0.363 (0.108)	0.307 (0.041)	0.532 (0.122)	0.173 (0.020)	0.435 (0.132)	1.309 (0.531)	0.413 (0.007)	0.451 (0.019)
DLinear	0.215 (0.016)	0.242 (0.009)	0.362 (0.009)	0.179 (0.004)	0.227 (0.006)	0.519 (0.008)	0.370 (0.000)	0.432 (0.001)
FILM	0.318 (0.010)	0.340 (0.011)	0.784 (0.064)	0.413 (0.010)	0.583 (0.008)	0.834 (0.031)	0.458 (0.001)	0.494 (0.003)
CSDI	0.102 (0.010)	0.539 (0.418)	0.238 (0.047)	0.231 (0.064)	0.151 (0.008)	1.483 (0.459)	0.252 (0.002)	0.408 (0.019)
US-GAN	0.137 (0.002)	0.264 (0.012)	0.296 (0.001)	0.151 (0.016)	0.458 (0.590)	0.938 (0.009)	0.310 (0.003)	0.358 (0.002)
GP-VAE	0.240 (0.006)	0.369 (0.012)	0.341 (0.007)	0.319 (0.010)	0.329 (0.017)	1.152 (0.074)	0.445 (0.006)	0.562 (0.004)
Mean	0.721	0.574	0.798	0.728	0.737	0.422	0.708	0.762
Median	0.681	0.518	0.778	0.667	0.71	0.408	0.69	0.747
LOCF	0.188	0.233	0.375	0.257	0.315	0.104	0.449	0.478
Linear	0.112	0.135	0.211	0.167	0.197	0.065	0.366	0.387

strategy and the training methodology from SAITS [20] are applied to reimplement them as imputation methods. Please refer to Appendix B and Appendix C.5 for more details of the benchmarked models as well as the systematic paradigm to leverage time series forecasting models for imputation purposes.

3.4 Implementation Details

Dataset Preprocessing: Except for Physionet2012, Physionet2019, and Pedestrian which contain separated time series samples already, all other datasets are split into the train, validation, and test sets according to the time period, then the sliding window function is applied to generate separated data samples. The standardization is applied to samples of all datasets. Refer to Appendix A.2 for more dataset preprocessing details. All preprocessed datasets are available on Google Drive at this link. **Missingness Patterns:** To make missing patterns diverse, we apply three different types of missingness (point, subsequence, and block) in our experiments. For the vivid illustration, please refer to C.1. **Evaluation Metrics:** MAE (mean absolute error), MSE (mean squared error), and MRE (mean relative error) are applied to evaluate the imputation performance. Their mathematical equations are put in Appendix C.2. Besides, inference time and the number of trainable parameters are also collected for discussion. **Hyper-parameter Optimization:** To obtain fair comparisons and conclusions, hyper-parameter optimization is performed for all deep-learning imputation algorithms. This functionality is implemented with PyPOTS [50] and NNI [69]. The details are available in Appendix C.3. **Downstream Task Design:** To explore how imputation affects downstream analysis, we perform various tasks with XGBoost, RNN, and Transformer on the imputed datasets for evaluation. Refer to Appendix C.4 for design details.

4 Experiments

In this section, we conduct a comprehensive analysis based on up to 34,804 experiments of 28 algorithms across 8 different domain datasets. Our experiments are divided into three main parts: (1) **Data Perspective:** We test different missingness ratios (10%, 50%, and 90%) and various missingness patterns (point, subsequence, block) across all datasets. (2) **Model Perspective:** We analyze all methods according to target task type (forecasting, imputation) and architecture type (Transformer/attention, RNN, CNN, MLP, etc.), while also considering the impact of model size and inference time on practical applications. (3) **Downstream Task Perspective:** We evaluate the imputed data quality using three different architectures (XGBoost, RNN, Transformer) across three classical time-series downstream tasks (classification, regression, and forecasting) to demonstrate the significance and importance of imputation in downstream tasks. Full results are listed in Appendix D.

		Performance of 50% block missing (MAE)					
		BeijingAir	ItalyAir	PeMS	ETT_I1	Electricity	Pedestrian
Transformer	→	0.42	0.49	0.46	0.51	1	0.64
SAITS	→	0.21	0.42	0.33	0.42	1.4	0.51
Nonstationary	→	0.3	0.42	0.69	0.51	0.35	0.61
ETSformer	→	0.3	0.56	0.77	0.65	1.3	0.65
PatchTST	→	0.3	0.5	0.39	0.56	1.2	0.62
Crossformer	→	0.26	0.46	0.41	0.52	1.2	0.61
Informr	→	0.21	0.44	0.35	0.46	1.3	0.55
Autoformer	→	0.69	0.95	0.63	1.1	1.4	0.88
Pyraformer	→	0.22	0.46	0.33	0.44	1.3	0.51
Transformer	→	0.2	0.4	0.35	0.44	1.4	0.53
BRITS	→	0.19	0.45	0.32	0.59	1.3	0.64
MRNN	→	0.71	0.8	0.67	0.8	1.9	0.77
GRUD	→	0.3	0.6	0.39	0.57	1.3	0.69
TimesNet	→	0.28	0.54	0.39	0.57	1.5	0.71
MiCN	→	0.49	0.72	0.6	0.71	1.5	—
SCINet	→	0.26	0.5	0.62	0.54	1.5	0.65
StemGNN	→	0.24	0.45	0.51	0.43	1.5	0.56
FreTS	→	0.26	0.49	0.45	0.5	1	0.63
Koopaa	→	0.31	0.48	0.62	0.56	1.9	0.62
DLinear	→	0.3	0.51	0.45	0.57	0.96	0.66
FLIM	→	0.35	0.49	0.77	0.65	1	0.59
CSDI	→	0.18	0.68	1.1	0.4	1.1	0.69
USGAN	→	0.22	0.48	0.39	0.81	1.3	0.66
GPVAE	→	0.29	0.56	0.37	0.65	1.3	0.72
Mean	→	0.71	0.62	0.83	0.72	0.43	0.77
Median	→	0.68	0.59	0.86	0.71	0.41	0.71
LOCF	→	0.4	0.49	0.7	0.72	0.25	0.74
Linear	→	0.28	0.38	0.72	0.53	0.14	0.55

Figure 3: Performance of 50% block missing.

		Performance of 50% subsequence missing (MAE)					
		BeijingAir	ItalyAir	PeMS	ETT_I1	Electricity	Pedestrian
Transformer	→	0.63	0.58	0.64	0.81	1.5	0.64
SAITS	→	0.22	0.39	0.35	0.64	1.4	0.51
Nonstationary	→	0.34	0.39	0.82	0.61	0.6	0.61
ETSformer	→	0.42	0.54	0.56	0.68	1.1	0.65
PatchTST	→	0.32	0.51	0.42	0.76	1.2	0.62
Crossformer	→	0.27	0.46	0.42	0.72	1.2	0.61
Informr	→	0.23	0.39	0.37	0.57	1.4	0.55
Autoformer	→	0.7	0.87	0.65	0.88	1.8	0.88
Pyraformer	→	0.23	0.41	0.35	0.67	1.4	0.51
Transformer	→	0.22	0.36	0.37	0.63	1.4	0.53
BRITS	→	0.19	0.41	0.33	0.73	1.2	0.64
MRNN	→	0.68	0.74	0.68	0.88	1.9	0.77
GRUD	→	0.34	0.59	0.4	0.76	1.2	0.69
TimesNet	→	0.31	0.54	0.41	0.73	1.4	0.71
MiCN	→	0.56	0.66	0.67	0.85	1.7	—
SCINet	→	0.27	0.48	0.67	0.71	1.3	0.65
StemGNN	→	0.28	0.43	0.5	0.63	1.5	0.56
FreTS	→	0.3	0.5	0.5	0.75	1.4	0.63
Koopaa	→	0.41	0.48	0.6	0.74	1.8	0.62
DLinear	→	0.31	0.51	0.46	0.76	1.2	0.66
FLIM	→	0.36	0.5	0.87	0.73	1.2	0.59
CSDI	→	0.21	0.48	0.62	0.56	0.92	0.69
USGAN	→	0.23	0.45	0.44	0.67	1.3	0.66
GPVAE	→	0.32	0.54	0.4	0.81	1.2	0.72
Mean	→	0.71	0.61	0.85	0.77	0.44	0.77
Median	→	0.68	0.55	0.89	0.78	0.41	0.71
LOCF	→	0.48	0.53	1.2	0.81	0.38	0.74
Linear	→	0.36	0.33	1	0.72	0.41	0.55

Figure 4: Performance of 50% subseq missing.

4.1 Data Perspective

We conduct the following three experiments on data and missingness patterns: datasets from different application domains, missingness rates, and different missing features.

Application Domain Table 1 shows that different models exhibit significant performance variations across datasets from different application domains. For instance, Autoformer performs well on the Pedestrian dataset (with an MAE of 0.197) but performs poorly on the ItalyAir dataset (with an MAE of 0.295). This trend is also observed within the same application domain. BRITS excels on the BeijingAir dataset (with an MAE of 0.127) but shows worse performance on the ItalyAir dataset (with an MAE of 0.235). Overall, different models demonstrate varying performance across different application domains and datasets, with each model having its own strengths and weaknesses in specific datasets. Even in simpler application fields, such as electricity, we can get better results using traditional LOCF and Linear methods. It seems that we cannot find a model that performs perfectly in all application scenarios.

Missingness Rate As the missingness data rate increases from 10% to 90%, there is a general trend of performance degradation across all models and datasets, as shown in Appendix D. For instance, Autoformer’s MAE on the BeijingAir dataset rises from 0.257 at 10% missingness to 0.898 at 50% and 0.806 at 90% missing. Different models exhibit varying sensitivity to missing data, with BRITS maintaining relatively lower errors compared to others, whereas CSDI shows extreme sensitivity. For example, CSDI’s MAE on the ItalyAir dataset jumps from 0.539 at 10% missingness to 4.492 at 90%. CSDI is a conditional diffusion model that performs poorly and becomes less stable with high missingness rates primarily due to noise accumulation, lack of contextual information, sparsity of training data, and uncertainty in the imputation targets. Computational time also varies, with CSDI showing substantially longer times at higher missingness rates, while models like Autoformer and DLinear remain consistent. We want to highlight the importance of selecting appropriate models based on the expected missing data rate. For models with similar performance, it is better to consider computational efficiency for practical implementation.

Missingness Pattern It is evident that different patterns significantly impact model performance, as indicated in Figures 3 and 4. Overall, block and subsequence missingness patterns result in higher error metrics compared to point missing, indicating that continuous missing data has a greater adverse effect on model performance. Specifically, point missingness has the least impact on most models, as they can easily interpolate or estimate the missing data from adjacent points; for example, BRITS performs excellently under this pattern. In contrast, block missingness leads to more significant information loss over extended periods, making it challenging for models to infer missing data from distant points, as seen with the increased MAE and MSE for Autoformer and Crossformer. Subsequence missingness further deteriorates model performance since the missing subsequences may contain critical time patterns or trends that the models cannot easily reconstruct. Thus, different missingness patterns affect model performance to varying degrees, with continuous missingness patterns (block and subsequence missing) posing greater challenges.

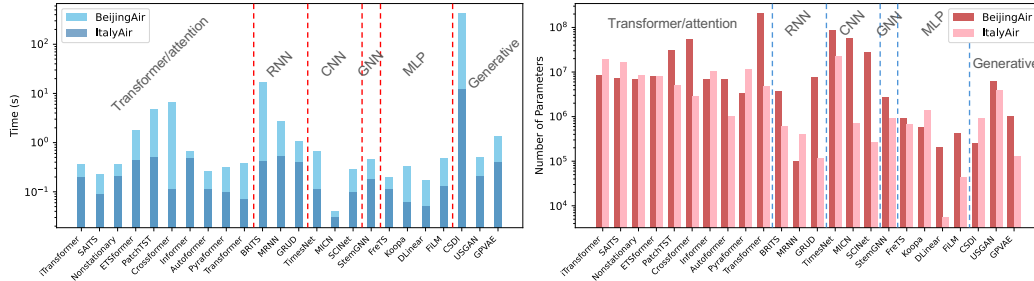


Figure 5: Inference time and the number of parameters on two air datasets with 10% point missing.

Remark 1: We suggest choosing imputation models tailored to the specific data characteristics, such as application domains, and missing patterns. Practitioners can leverage our comprehensive insights to make informed model choices to narrow their trials and experiments in selecting models, enhancing the development and open-source accessibility of time series imputation.

4.2 Model Perspective

Due to the space limit, we limit our discussions in this section to the model architectures and the original task based on 10% missingness rate.

Architecture By analyzing the inference time, model size, and performance metrics of different architectures from Figure 5 and Table 1, we can draw the following conclusions: Transformer/Attention-based models, such as Autoformer and Informer, demonstrate excellent performance, but some models like Crossformer and SAITS have larger model sizes, potentially leading to lower inference efficiency. RNN-based models like BRITS show good performance (low MSE, MAE) but have longer inference times and moderate model sizes. CNN-based models like SCINet have faster inference times but relatively larger model sizes, with slightly lower performance compared to Transformer and RNN architectures. MLP-based models like DLinear have clear advantages in inference time and model size, with moderate performance, making them suitable for applications requiring quick inference and smaller models. CSDI, as a generative model, performs well on some metrics (e.g., MAE) but has extremely long inference time and moderate model size, suitable for scenarios demanding very high performance. Traditional methods, due to their limited scope, usually do not yield optimal results, especially in datasets with high missingness rates and complexity. However, they can be more efficient and perform better on simpler datasets. In summary, different architecture models have their own strengths and weaknesses in terms of inference time, model size, and performance metrics, necessitating the selection of an appropriate model based on specific application requirements.

Forecasting Backbones for Imputation With the adaptation paradigm C.5, we transfer the backbone of the time series forecasting models to the imputation task and compare their performance against typical imputation methods. Results are categorized into Table 1, and the detailed descriptions of the backbones are discussed in Appendix B. For forecasting backbones, Crossformer has a longer inference time of 6.77 seconds, a larger model size of 52,933,788, but stable performance, with an MAE of 0.184 on the Beijing dataset. DLinear, with the shortest inference time of 0.17 seconds and a model size of 204,728, shows efficient performance with an MAE of 0.215 on the Beijing dataset, making it ideal for real-time applications. In imputation, BRITS has an inference time of 17.04 seconds, a model size of 3,598,496, and performs excellently on the Beijing dataset with an MAE of 0.127. CSDI, however, has a long inference time of 417.52 seconds, a model size of 244,833, and higher MSE values, limiting its practical use despite advanced techniques. Generally, methods originally designed for imputation do not exhibit extraordinary performance compared to those designed for forecasting. In many scenarios, the adapted forecasting methods tend to perform better. A potential reason is that there are more papers on time series forecasting, compared to time series imputation. Therefore, models in time series forecasting are more updated and advanced in capturing temporal information and multivariate correlations. The experimental results demonstrate the success of our adaptation paradigm.

Remark 2: Existing forecasting backbones can be effectively applied to imputation tasks, enhancing the interaction between different time series tasks. This suggests that the imputation field can benefit from leveraging techniques and models originally designed for forecasting and other time series tasks.

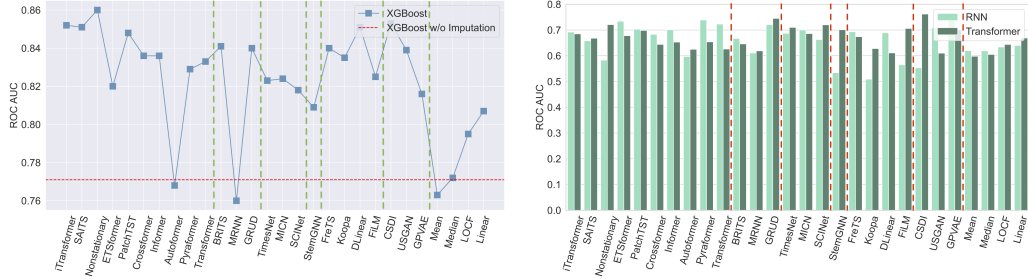


Figure 6: Comparison of downstream classification performance on the PhysioNet2012 dataset with 10% point missing data.

This cross-application improves the versatility and efficiency of time series models, opening new avenues for research and practical applications.

4.3 Downstream Tasks Perspective

Classification Task In this ablation test, we first apply different models performing the imputation task then conduct the classification task based on three types of classifiers. We would like to explore the performance improvement of various imputation methods for the downstream classification task, as shown in Figure 6. For example, iTransformer shows a ROC_AUC of 0.771 without imputation, which improves significantly to 0.852 after imputation. Besides, the nonstationary method performs best with imputation, achieving a ROC_AUC of 0.860, demonstrating strong robustness in handling missing data and positively contributing to downstream tasks. Overall, imputation plays a crucial role in the classification task for preprocessing, as the performance of most methods significantly improving after imputation. Also, selecting an appropriate imputation method can enhance downstream performance. Therefore, future research and applications might place greater emphasis on the development and optimization of imputation techniques to improve the robustness and effect of various downstream classification algorithms.

Regression Task As described in Table 2, imputation methods with different missingness patterns (50% point, subsequence, and block missing) significantly affect the performance of downstream regression tasks. For instance, the BRITS model, which is an RNN-based method, achieves the lowest MAE of 0.826 in the block missingness scenario, indicating its robustness in maintaining data integrity and its effectiveness in supporting accurate regression outcomes. This suggests that the

Table 2: Regression performance comparison in ETT_h1 datasets with 50% point missing, 50% block missing and 50% subsequence missing.

	ETT_h1 (point 50%)			ETT_h1 (subsequence 50%)			ETT_h1 (block 50%)		
	XGB	RNN	Transformer	XGB	RNN	Transformer	XGB	RNN	Transformer
iTransformer	1.224 (0.000)	1.377 (0.062)	1.406 (0.069)	1.170 (0.000)	1.434 (0.047)	1.470 (0.053)	1.208 (0.000)	1.422 (0.075)	1.399 (0.080)
SAITS	1.175 (0.000)	1.402 (0.056)	1.401 (0.083)	1.094 (0.000)	1.424 (0.077)	1.469 (0.054)	1.168 (0.000)	1.363 (0.072)	1.385 (0.057)
Nonstationary	1.227 (0.000)	1.446 (0.061)	1.384 (0.087)	1.284 (0.000)	1.448 (0.053)	1.469 (0.036)	1.189 (0.000)	1.438 (0.059)	1.368 (0.055)
PatchTST	1.222 (0.000)	1.329 (0.060)	1.351 (0.061)	1.187 (0.000)	1.407 (0.059)	1.433 (0.058)	1.004 (0.000)	1.285 (0.064)	1.327 (0.096)
ETSformer	1.234 (0.000)	1.398 (0.059)	1.370 (0.074)	1.253 (0.000)	1.476 (0.079)	1.502 (0.042)	1.183 (0.000)	1.362 (0.078)	1.340 (0.074)
Crossformer	1.228 (0.000)	1.391 (0.058)	1.380 (0.070)	1.145 (0.000)	1.449 (0.058)	1.474 (0.042)	1.149 (0.000)	1.335 (0.070)	1.285 (0.081)
Informer	1.214 (0.000)	1.391 (0.059)	1.398 (0.076)	1.196 (0.000)	1.423 (0.076)	1.442 (0.042)	1.158 (0.000)	1.333 (0.080)	1.351 (0.055)
Autoformer	1.348 (0.000)	1.450 (0.108)	1.442 (0.155)	1.364 (0.000)	1.471 (0.061)	1.538 (0.072)	1.327 (0.000)	1.267 (0.047)	1.363 (0.204)
Pyraformer	1.169 (0.000)	1.366 (0.057)	1.373 (0.071)	1.081 (0.000)	1.391 (0.077)	1.443 (0.042)	1.071 (0.000)	1.328 (0.069)	1.330 (0.053)
Transformer	1.170 (0.000)	1.378 (0.056)	1.357 (0.081)	1.074 (0.000)	1.391 (0.060)	1.350 (0.090)	1.128 (0.000)	1.296 (0.064)	1.277 (0.077)
BRITS	1.177 (0.000)	1.371 (0.061)	1.364 (0.076)	0.999 (0.000)	1.153 (0.042)	1.146 (0.036)	0.826 (0.000)	1.024 (0.010)	1.000 (0.057)
MRNN	1.070 (0.000)	1.250 (0.076)	1.379 (0.058)	1.111 (0.000)	1.362 (0.061)	1.483 (0.055)	0.870 (0.000)	1.274 (0.078)	1.387 (0.053)
GRUD	1.205 (0.000)	1.339 (0.061)	1.326 (0.074)	1.123 (0.000)	1.351 (0.058)	1.362 (0.044)	1.043 (0.000)	1.286 (0.046)	1.211 (0.080)
TimesNet	1.127 (0.000)	1.333 (0.054)	1.316 (0.066)	1.213 (0.000)	1.446 (0.058)	1.460 (0.041)	1.064 (0.000)	1.316 (0.068)	1.294 (0.101)
MICN	1.163 (0.000)	1.305 (0.078)	1.379 (0.070)	1.121 (0.000)	1.442 (0.052)	1.503 (0.060)	1.145 (0.000)	1.338 (0.066)	1.344 (0.073)
SCINet	1.174 (0.000)	1.411 (0.055)	1.375 (0.080)	1.181 (0.000)	1.450 (0.061)	1.446 (0.038)	1.182 (0.000)	1.361 (0.075)	1.323 (0.065)
StemGNN	1.139 (0.000)	1.392 (0.057)	1.410 (0.078)	1.211 (0.000)	1.391 (0.067)	1.439 (0.045)	1.136 (0.000)	1.373 (0.064)	1.323 (0.052)
FreTS	1.207 (0.000)	1.406 (0.056)	1.397 (0.082)	1.159 (0.000)	1.456 (0.079)	1.514 (0.045)	1.163 (0.000)	1.356 (0.080)	1.355 (0.068)
Koopa	1.227 (0.000)	1.384 (0.064)	1.419 (0.062)	1.233 (0.000)	1.446 (0.083)	1.509 (0.046)	1.274 (0.000)	1.347 (0.063)	1.302 (0.052)
DLinear	1.216 (0.000)	1.380 (0.056)	1.397 (0.076)	1.212 (0.000)	1.466 (0.058)	1.512 (0.044)	1.166 (0.000)	1.368 (0.064)	1.359 (0.114)
FILM	1.247 (0.000)	1.379 (0.057)	1.442 (0.048)	1.422 (0.000)	1.389 (0.057)	1.455 (0.036)	1.301 (0.000)	1.391 (0.057)	1.368 (0.060)
CSDI	1.136 (0.000)	1.373 (0.050)	1.393 (0.070)	1.191 (0.000)	1.354 (0.049)	1.413 (0.041)	1.202 (0.000)	1.355 (0.048)	1.362 (0.054)
US-GAN	1.155 (0.000)	1.299 (0.040)	1.283 (0.055)	1.004 (0.000)	1.244 (0.052)	1.219 (0.079)	0.951 (0.000)	1.174 (0.069)	1.098 (0.145)
GP-VAE	1.178 (0.000)	1.336 (0.066)	1.340 (0.076)	1.138 (0.000)	1.310 (0.046)	1.354 (0.077)	0.996 (0.000)	1.177 (0.061)	1.184 (0.077)
Mean	1.431 (0.000)	1.512 (0.120)	1.627 (0.072)	1.430 (0.000)	1.859 (0.095)	1.779 (0.035)	1.413 (0.000)	1.669 (0.083)	1.750 (0.043)
Median	1.517 (0.086)	1.531 (0.128)	1.671 (0.069)	1.499 (0.069)	1.858 (0.089)	1.777 (0.034)	1.496 (0.083)	1.688 (0.100)	1.736 (0.061)
LOCF	1.446 (0.123)	1.477 (0.134)	1.571 (0.158)	1.446 (0.094)	1.699 (0.237)	1.651 (0.182)	1.433 (0.112)	1.601 (0.150)	1.611 (0.188)
Linear	1.393 (0.140)	1.453 (0.127)	1.525 (0.163)	1.423 (0.091)	1.610 (0.258)	1.588 (0.193)	1.395 (0.118)	1.558 (0.151)	1.556 (0.191)

ability of BRITS to capture temporal dependencies despite substantial data loss translates into more reliable regression predictions. Similarly, Transformer-based models like Autoformer and Informer demonstrate strong performance, with MAE values of 1.327 and 1.158 respectively in the block missingness scenario, highlighting their effectiveness in handling complex missing data patterns and enhancing the predictive accuracy of downstream regression tasks. Conversely, traditional imputation methods such as Mean and Median show higher MAE values, 1.413 and 1.496 respectively, in the same scenario, underscoring their limitations and resulting in less accurate regression results. The performance of a simple XGBoost model applied to imputed data, which outperforms untuned deep learning classifiers, further reinforces the importance of robust imputation. This demonstrates that high-quality imputation not only preserves the integrity of the data but also significantly enhances the predictive power of regression models.

We also perform experiments that take forecasting as a downstream task in Appendix D.7.3.

Remark 3: Imputation is not only crucial in itself but also plays a vital role in enhancing the performance of downstream tasks, such as classification, regression, and forecasting. By filling in missing data, imputation helps in recovering the original temporal information of the original dataset, which is beneficial for reliable analysis and modeling.

5 Conclusion

In this paper, we introduce TSI-Bench, a comprehensive benchmark for time series imputation. Our evaluation of 28 algorithms on 8 real-world datasets demonstrates that successful data imputation depends on various factors, including the deep learning structures, missingness rates and patterns across space-time, and the datasets themselves. Although this process is complex, our benchmark suite and experimental results can serve as a reference for future research, and provide practical imputation guidelines in real scenarios.

We envision TSI-Bench as a long-term evolving project and are committed to its continuous development. Our future roadmap includes integrating more advanced deep-learning models and expanding the range of datasets. Additionally, we aim to enhance the user-friendliness of TSI-Bench, with the goal of establishing it as a prevalent tool for time series imputation.

Acknowledgments and Disclosure of Funding

We thank King’s College London for providing computing resources.

References

- [1] Kexin Zhang, Qingsong Wen, Chaoli Zhang, Rongyao Cai, Ming Jin, Yong Liu, James Y Zhang, Yuxuan Liang, Guansong Pang, Dongjin Song, and Shirui Pan. Self-supervised learning for time series analysis: Taxonomy, progress, and prospects. *IEEE Transactions on Pattern Analysis and Machine Intelligence*, 2024.
- [2] Ming Jin, Yifan Zhang, Wei Chen, Kexin Zhang, Yuxuan Liang, Bin Yang, Jindong Wang, Shirui Pan, and Qingsong Wen. Position: What can large language models tell us about time series analysis. In *ICML*, 2024.
- [3] James D Hamilton. *Time series analysis*. Princeton university press, 2020.
- [4] Ya Liu, Yingjie Zhou, Kai Yang, and Xin Wang. Unsupervised deep learning for iot time series. *IEEE Internet of Things Journal*, 10(16):14285–14306, 2023.
- [5] Yuxuan Liang, Yutong Xia, Songyu Ke, Yiwei Wang, Qingsong Wen, Junbo Zhang, Yu Zheng, and Roger Zimmermann. Airformer: Predicting nationwide air quality in china with transformers. In *Proceedings of the AAAI Conference on Artificial Intelligence*, volume 37, pages 14329–14337, 2023.
- [6] Zhaoyang Zhu, Weiqi Chen, Rui Xia, Tian Zhou, Peisong Niu, Bingqing Peng, Wenwei Wang, Hengbo Liu, Ziqing Ma, Xinyue Gu, et al. Energy forecasting with robust, flexible, and explainable machine learning algorithms. *AI Magazine*, 44(4):377–393, 2023.
- [7] Zeng Zeng, Wei Zhao, Peisheng Qian, Yingjie Zhou, Ziyuan Zhao, Cen Chen, and Cuntai Guan. Robust traffic prediction from spatial–temporal data based on conditional distribution learning. *IEEE Transactions on Cybernetics*, 52(12):13458–13471, 2022.
- [8] Zina M Ibrahim, Daniel Bean, Thomas Searle, Linglong Qian, Honghan Wu, Anthony Shek, Zeljko Kraljevic, James Galloway, Sam Norton, James TH Teo, et al. A knowledge distillation ensemble framework for predicting short-and long-term hospitalization outcomes from electronic health records data. *IEEE Journal of Biomedical and Health Informatics*, 26(1):423–435, 2021.
- [9] Chenguang Fang and Chen Wang. Time series data imputation: A survey on deep learning approaches. *arXiv preprint arXiv:2011.11347*, 2020.
- [10] Jun Wang, Wenjie Du, Wei Cao, Keli Zhang, Wenjia Wang, Yuxuan Liang, and Qingsong Wen. Deep learning for multivariate time series imputation: A survey. *arXiv preprint arXiv:2402.04059*, 2024.
- [11] Linglong Qian, Zina Ibrahim, Wenjie Du, Yiyuan Yang, and Richard JB Dobson. Unveiling the secrets: How masking strategies shape time series imputation. *arXiv preprint arXiv:2405.17508*, 2024.
- [12] Jinsung Yoon, William R. Zame, and Mihaela van der Schaar. Estimating missing data in temporal data streams using multi-directional recurrent neural networks. *IEEE Trans. on Biomedical Engineering*, 2019.
- [13] Haixu Wu, Tengge Hu, Yong Liu, Hang Zhou, Jianmin Wang, and Mingsheng Long. TimesNet: Temporal 2D-Variation Modeling for General Time Series Analysis. In *ICLR*, 2023.
- [14] Andrea Cini, Ivan Marisca, and Cesare Alippi. Filling the g_ap_s: Multivariate time series imputation by graph neural networks. In *ICLR*, 2022.
- [15] Ivan Marisca, Andrea Cini, and Cesare Alippi. Learning to reconstruct missing data from spatiotemporal graphs with sparse observations. *NeurIPS*, 2022.
- [16] Jiawei Ma, Zheng Shou, Alireza Zareian, Hassan Mansour, Anthony Vetro, and Shih-Fu Chang. CDSA: cross-dimensional self-attention for multivariate, geo-tagged time series imputation. *arXiv preprint arXiv:1905.09904*, 2019.
- [17] Parikshit Bansal, Prathamesh Deshpande, and Sunita Sarawagi. Missing value imputation on multidimensional time series. In *VLDB*, 2021.
- [18] Zhengping Che, Sanjay Purushotham, Kyunghyun Cho, David Sontag, and Yan Liu. Recurrent neural networks for multivariate time series with missing values. *Scientific Reports*, 8(1), Apr 2018.

- [19] Wei Cao, Dong Wang, Jian Li, Hao Zhou, Lei Li, and Yitan Li. Brits: Bidirectional recurrent imputation for time series. *NeurIPS*, 2018.
- [20] Wenjie Du, David Cote, and Yan Liu. SAITS: Self-Attention-based Imputation for Time Series. *Expert Systems with Applications*, 219:119619, 2023.
- [21] Ahmad Wisnu Mulyadi, Eunji Jun, and Heung-II Suk. Uncertainty-aware variational-recurrent imputation network for clinical time series. *IEEE Transactions on Cybernetics*, 52(9):9684–9694, 2021.
- [22] Seunghyun Kim, Hyunsu Kim, Eunggu Yun, Hwangrae Lee, Jaehun Lee, and Juho Lee. Probabilistic imputation for time-series classification with missing data. In *ICML*, 2023.
- [23] Yonghong Luo, Xiangrui Cai, Ying ZHANG, Jun Xu, and Yuan xiaojie. Multivariate time series imputation with generative adversarial networks. In *NeurIPS*, 2018.
- [24] Yonghong Luo, Ying Zhang, Xiangrui Cai, and Xiaojie Yuan. E²GAN: End-to-end generative adversarial network for multivariate time series imputation. In *IJCAI*, 2019.
- [25] Juan Lopez Alcaraz and Nils Strodthoff. Diffusion-based time series imputation and forecasting with structured state space models. *Transactions on Machine Learning Research*, 2023.
- [26] Yu Chen, Wei Deng, Shikai Fang, Fengpei Li, Nicole Tianjiao Yang, Yikai Zhang, et al. Provably convergent schrödinger bridge with applications to probabilistic time series imputation. In *ICML*, 2023.
- [27] Yiyuan Yang, Ming Jin, Haomin Wen, Chaoli Zhang, Yuxuan Liang, Lintao Ma, Yi Wang, Chenghao Liu, Bin Yang, Zenglin Xu, et al. A survey on diffusion models for time series and spatio-temporal data. *arXiv preprint arXiv:2404.18886*, 2024.
- [28] Vincent Fortuin, Dmitry Baranchuk, Gunnar Rätsch, and Stephan Mandt. Gp-vae: Deep probabilistic time series imputation. In *International conference on artificial intelligence and statistics*, pages 1651–1661. PMLR, 2020.
- [29] Xiaoye Miao, Yangyang Wu, Jun Wang, Yunjun Gao, Xudong Mao, and Jianwei Yin. Generative semi-supervised learning for multivariate time series imputation. In *AAAI*, 2021.
- [30] Yusuke Tashiro, Jiaming Song, Yang Song, and Stefano Ermon. CSDI: Conditional score-based diffusion models for probabilistic time series imputation. In *NeurIPS*, 2021.
- [31] Haixu Wu, Jiehui Xu, Jianmin Wang, and Mingsheng Long. Autoformer: Decomposition transformers with auto-correlation for long-term series forecasting. *Advances in neural information processing systems*, 34:22419–22430, 2021.
- [32] Haoyi Zhou, Shanghang Zhang, Jieqi Peng, Shuai Zhang, Jianxin Li, Hui Xiong, and Wancai Zhang. Informer: Beyond efficient transformer for long sequence time-series forecasting. In *The Thirty-Fifth AAAI Conference on Artificial Intelligence, AAAI 2021, Virtual Conference*, volume 35, pages 11106–11115. AAAI Press, 2021.
- [33] Yuqi Nie, Nam H. Nguyen, Phanwadee Sinthong, and Jayant Kalagnanam. A time series is worth 64 words: Long-term forecasting with transformers. In *Proceedings of the International Conference on Learning Representations*, 2023.
- [34] Defu Cao, Yujing Wang, Juanyong Duan, Ce Zhang, Xia Zhu, Congrui Huang, Yunhai Tong, Bixiong Xu, Jing Bai, Jie Tong, et al. Spectral temporal graph neural network for multivariate time-series forecasting. *Advances in Neural Information Processing Systems*, 33:17766–17778, 2020.
- [35] Zonghan Wu, Shirui Pan, Guodong Long, Jing Jiang, Xiaojun Chang, and Chengqi Zhang. Connecting the dots: Multivariate time series forecasting with graph neural networks. In *Proceedings of the 26th ACM SIGKDD International Conference on Knowledge Discovery & Data Mining*, 2020.
- [36] Yijing Liu, Qinxian Liu, Jian-Wei Zhang, Haozhe Feng, Zhongwei Wang, Zihan Zhou, and Wei Chen. Multivariate time-series forecasting with temporal polynomial graph neural networks. *Advances in neural information processing systems*, 35:19414–19426, 2022.
- [37] Ming Jin, Huan Yee Koh, Qingsong Wen, Daniele Zambon, Cesare Alippi, Geoffrey I Webb, Irwin King, and Shirui Pan. A survey on graph neural networks for time series: Forecasting, classification, imputation, and anomaly detection. *arXiv preprint arXiv:2307.03759*, 2023.

- [38] Vijay Ekambaram, Arindam Jati, Nam Nguyen, Phanwadee Sinthong, and Jayant Kalagnanam. Tsmixer: Lightweight mlp-mixer model for multivariate time series forecasting. *arXiv preprint:2306.09364*, 2023.
- [39] Si-An Chen, Chun-Liang Li, Nate Yoder, Sercan O Arik, and Tomas Pfister. Tsmixer: An all-mlp architecture for time series forecasting. *arXiv preprint:2303.06053*, 2023.
- [40] Zepu Wang, Yuqi Nie, Peng Sun, Nam H Nguyen, John Mulvey, and H Vincent Poor. St-mlp: A cascaded spatio-temporal linear framework with channel-independence strategy for traffic forecasting. *arXiv preprint arXiv:2308.07496*, 2023.
- [41] Qingsong Wen, Tian Zhou, Chaoli Zhang, Weiqi Chen, Ziqing Ma, Junchi Yan, and Liang Sun. Transformers in time series: a survey. In *Proceedings of the Thirty-Second International Joint Conference on Artificial Intelligence*, pages 6778–6786, 2023.
- [42] Haoyi Zhou, Shanghang Zhang, Jieqi Peng, Shuai Zhang, Jianxin Li, Hui Xiong, and Wancai Zhang. Informer: Beyond efficient transformer for long sequence time-series forecasting. In *Proceedings of the AAAI Conference on Artificial Intelligence*, number 12, pages 11106–11115, 2021.
- [43] Yunhao Zhang and Junchi Yan. Crossformer: Transformer utilizing cross-dimension dependency for multivariate time series forecasting. In *ICLR*, 2022.
- [44] Ailing Zeng, Muxi Chen, Lei Zhang, and Qiang Xu. Are transformers effective for time series forecasting? In *Proceedings of the AAAI Conference on Artificial Intelligence*, number 9, pages 11121–11128, 2023.
- [45] Ilya O Tolstikhin, Neil Houlsby, Alexander Kolesnikov, Lucas Beyer, Xiaohua Zhai, Thomas Unterthiner, Jessica Yung, Andreas Steiner, Daniel Keysers, Jakob Uszkoreit, et al. Mlp-mixer: An all-mlp architecture for vision. *Advances in Neural Information Processing Systems*, 34:24261–24272, 2021.
- [46] Yong Liu, Chenyu Li, Jianmin Wang, and Mingsheng Long. Koopa: Learning non-stationary time series dynamics with koopman predictors. *arXiv preprint:2305.18803*, 2023.
- [47] Zhijian Xu, Ailing Zeng, and Qiang Xu. Fits: Modeling time series with 10k parameters. *arXiv preprint:2307.03756*, 2023.
- [48] Qingsong Wen, Jingkun Gao, Xiaomin Song, Liang Sun, Huan Xu, and Shenghuo Zhu. Robust-stl: A robust seasonal-trend decomposition algorithm for long time series. In *Proceedings of the AAAI conference on artificial intelligence*, volume 33, pages 5409–5416, 2019.
- [49] Zepu Wang, Dingyi Zhuang, Yankai Li, Jinhua Zhao, and Peng Sun. St-gin: An uncertainty quantification approach in traffic data imputation with spatio-temporal graph attention and bidirectional recurrent united neural networks. *arXiv preprint: 2305.06480*, 2023.
- [50] Wenjie Du. PyPOTS: a Python toolbox for data mining on Partially-Observed Time Series. 2023.
- [51] Shuyi Zhang, Bin Guo, Anlan Dong, Jing He, Ziping Xu, and Song Xi Chen. Cautionary tales on air-quality improvement in beijing. *Proceedings of the Royal Society A: Mathematical, Physical and Engineering Sciences*, 473(2205):20170457, 2017.
- [52] Saverio De Vito, Ettore Massera, Marco Piga, Luca Martinotto, and Girolamo Di Francia. On field calibration of an electronic nose for benzene estimation in an urban pollution monitoring scenario. *Sensors and Actuators B: Chemical*, 129(2):750–757, 2008.
- [53] Wensi Tang, Lu Liu, and Guodong Long. Interpretable time-series classification on few-shot samples. In *2020 International Joint Conference on Neural Networks (IJCNN)*, pages 1–8. IEEE, 2020.
- [54] Ikaro Silva, George Moody, Daniel J Scott, Leo A Celi, and Roger G Mark. Predicting in-hospital mortality of icu patients: The physionet/computing in cardiology challenge 2012. In *2012 Computing in Cardiology*, pages 245–248. IEEE, 2012.
- [55] Matthew A Reyna, Christopher S Josef, Russell Jeter, Supreeth P Shashikumar, M Brandon Westover, Shamim Nemati, Gari D Clifford, and Ashish Sharma. Early prediction of sepsis from clinical data: the physionet/computing in cardiology challenge 2019. *Critical care medicine*, 48(2):210–217, 2020.

- [56] A. Yarkin Yıldız, Emirhan Koç, and Aykut Koç. Multivariate time series imputation with transformers. *IEEE Signal Processing Letters*, 29:2517–2521, 2022.
- [57] Shizhan Liu, Hang Yu, Cong Liao, Jianguo Li, Weiyao Lin, Alex X Liu, and Schahram Dustdar. Pyraformer: Low-complexity pyramidal attention for long-range time series modeling and forecasting. In *Proceedings of the International Conference on Learning Representations*, 2021.
- [58] Gerald Woo, Chenghao Liu, Doyen Sahoo, Akshat Kumar, and Steven Hoi. Etsformer: Exponential smoothing transformers for time-series forecasting. *arXiv preprint arXiv:2202.01381*, 2022.
- [59] Yong Liu, Haixu Wu, Jianmin Wang, and Mingsheng Long. Non-stationary transformers: Exploring the stationarity in time series forecasting. *Advances in Neural Information Processing Systems*, 35:9881–9893, 2022.
- [60] Yong Liu, Tengge Hu, Haoran Zhang, Haixu Wu, Shiyu Wang, Lintao Ma, and Mingsheng Long. itransformer: Inverted transformers are effective for time series forecasting. *arXiv preprint arXiv:2310.06625*, 2023.
- [61] Jinsung Yoon, William R Zame, and Mihaela van der Schaar. Estimating missing data in temporal data streams using multi-directional recurrent neural networks. *IEEE Transactions on Biomedical Engineering*, 66(5):1477–1490, 2018.
- [62] Zhengping Che, Sanjay Purushotham, Kyunghyun Cho, David Sontag, and Yan Liu. Recurrent neural networks for multivariate time series with missing values. *Scientific reports*, 8(1):6085, 2018.
- [63] Huiqiang Wang, Jian Peng, Feihu Huang, Jince Wang, Junhui Chen, and Yifei Xiao. Micn: Multi-scale local and global context modeling for long-term series forecasting. In *The Eleventh International Conference on Learning Representations*, 2022.
- [64] Minhao Liu, Ailing Zeng, Muxi Chen, Zhijian Xu, Qiuxia Lai, Lingna Ma, and Qiang Xu. Scinet: Time series modeling and forecasting with sample convolution and interaction. *Advances in Neural Information Processing Systems*, 35:5816–5828, 2022.
- [65] Tian Zhou, Ziqing Ma, Qingsong Wen, Liang Sun, Tao Yao, Wotao Yin, Rong Jin, et al. Film: Frequency improved legendre memory model for long-term time series forecasting. *Advances in Neural Information Processing Systems*, 35:12677–12690, 2022.
- [66] Yong Liu, Chenyu Li, Jianmin Wang, and Mingsheng Long. Koopa: Learning non-stationary time series dynamics with koopman predictors. *Advances in Neural Information Processing Systems*, 36, 2024.
- [67] Kun Yi, Qi Zhang, Wei Fan, Shoujin Wang, Pengyang Wang, Hui He, Ning An, Defu Lian, Longbing Cao, and Zhendong Niu. Frequency-domain mlps are more effective learners in time series forecasting. *Advances in Neural Information Processing Systems*, 36, 2024.
- [68] Xiaoye Miao, Yangyang Wu, Jun Wang, Yunjun Gao, Xudong Mao, and Jianwei Yin. Generative semi-supervised learning for multivariate time series imputation. In *Proceedings of the AAAI conference on artificial intelligence*, volume 35, pages 8983–8991, 2021.
- [69] Microsoft. Neural Network intelligence.
- [70] Mohammed Saeed, Mauricio Villarroel, Andrew T Reisner, Gari Clifford, Li-Wei Lehman, George Moody, Thomas Heldt, Tin H Kyaw, Benjamin Moody, and Roger G Mark. Multiparameter intelligent monitoring in intensive care ii: a public-access intensive care unit database. *Critical care medicine*, 39(5):952–960, 2011.
- [71] Ashish Vaswani, Noam Shazeer, Niki Parmar, Jakob Uszkoreit, Llion Jones, Aidan N Gomez, et al. Attention is all you need. In *NeurIPS*, 2017.
- [72] King’s College London. King’s computational research, engineering and technology environment (create), 2022. Retrieved March 2, 2022.

A Detailed Description of Datasets and Preprocessing

A.1 Datasets for evaluation

Detailed descriptions of the eight used datasets are listed below. An overview of the datasets’ general information is presented in Table 3.

Table 3: General information of the eight datasets used in this work.

Dataset	Air		Traffic		Electricity		Healthcare	
	BeijingAir	ItalyAir	PeMS	Pedestrian	ETTh1	Electricity	PhysioNet2012	PhysioNet2019
# of Total Samples	1458	774	727	3633	358	1457	3997	4927
# of Variables	132	13	862	1	7	370	35	33
Sample Sequence Length	24	12	24	24	48	96	48	48
Time Interval	1H	1H	1H	1H	1H	15Min	1H	1H
Original Missing Rate (%)	1.6	0	0	0	0	0	79.3	73.9
Train Dataset Length	851	466	455	955	212	851	2557	3152
Validation Dataset Length	304	154	122	239	75	304	640	789
Test Dataset Length	303	154	150	2439	71	302	800	986

A.1.1 Air quality datasets

- **BeijingAir**² [51]: BeijingAir dataset includes hourly air pollutants data from 12 nationally-controlled air-quality monitoring sites from March 2013 to February 2017. The dataset contains 420,768 instances, with 6 main air pollutants and 6 relevant meteorological variables at multiple sites in Beijing. We aggregate these variables from all sites together so this dataset has $12*12=132$ features.
- **ItalyAir**³ [52]: ItalyAir dataset contains 9358 instances of hourly averaged responses of 5 metal oxides from chemical sensors, along with hourly averaged concentrations of 7 pollutants from certified analyzers, from March 2004 to February 2005.

A.1.2 Traffic datasets

- **PeMS**⁴: The PeMS is a collection of hourly data from California Department of Transportation, which describes the road occupancy rates measured by different sensors on San Francisco Bay area freeways.
- **Pedestrian**⁵ [53]: The City of Melbourne, Australia has developed an automated pedestrian counting system to better understand pedestrian activity within the municipality, The data of a specific region is from the whole year of 2017.

A.1.3 Electricity datasets

- **Electricity**⁶: The Electricity Load Diagrams dataset contains hourly electricity consumption (kWh) for 370 clients over the period from January 2011 to December 2014.
- **ETT**⁷ [32]: The ETT dataset, collected from power transformers, includes preprocessed data on power load and oil temperature from July 2016 to July 2018. In the experiments, we use ETTh1 included in ETT.

A.1.4 Healthcare datasets

- **PhysioNet2012**⁸ [54]: The PhysioNet/Computing in Cardiology Challenge 2012 dataset includes 12,000 ICU patient records from the MIMIC II Clinical database, version 2.6 [70], focusing on patient-specific prediction of in-hospital mortality using data from the first 48

²<https://archive.ics.uci.edu/dataset/501/beijing+multi+site+air+quality+data>

³<https://archive.ics.uci.edu/dataset/360/air+quality>

⁴<https://PeMS.dot.ca.gov>

⁵<https://www.timeseriesclassification.com/description.php?Dataset=MelbournePedestrian>

⁶<https://archive.ics.uci.edu/dataset/321/electricityloadaddiagrams20112014>

⁷<https://github.com/zhouhaoyi/ETDataset>

⁸<https://physionet.org/content/challenge-2012/1.0.0/>

hours of ICU admission. Not all variables are available in all cases, hence about 80% values are missing in this dataset. The whole dataset has three subsets, and we only use the subset A in our experiments.

- **PhysioNet2019**⁹ [55]: The PhysioNet Challenge 2019 dataset includes clinical data from ICU patients across three hospitals, with a total of 40,336 patient records and 40 clinical and physiological variables for each patient. Note that this dataset has two subsets, and we only use the subset A in our setting.

A.2 Datasets Preprocessing Details

BeijingAir, ItalyAir, PeMS, Electricity, and ETT_h1 are all long time series continuously collected from certain sources. Therefore, to generate them into the train, validation, and test sets and to avoid data leakage, we should first split them according to the time period. In BeijingAir, the first 28 months (2013/03 - 2015/06) of data are taken for training, the following 10 months (2015/07 - 2016/04) are for validation, and the left 10 months (2016/05 - 2017/02) are for test. In PeMS, the training set takes the first 15 months (2016/07 - 2017/09) of data, and the validation set and test set take the following 4 months (2017/10 - 2018/01) and 6 months (2018/02 - 2018/07) respectively. Electricity uses the first 10 months (2011/01 - 2011/10) as the test set, the following 10 months (2011/11 - 2012/08) for validation, and the last 28 months (2012/09 - 2014/12) for training. The training, validation, and test sets of ETT_h1 separately take the first 14 months (2016/07 - 2017/08), the following 5 months (2017/09 - 2018/01), and the last 5 months (2018/02 - 2018/06). ItalyAir is split into 60%, 20%, and 20% for training, validation, and test. The sliding window function is applied to these five datasets to produce data samples. The window size of ItalyAir is 12, and 24 for BeijingAir and PeMS, 48 for ETT_h1, 96 for Electricity. The sliding length is kept the same as the window size to guarantee there is no overlap between generated samples.

Dataset Pedestrian is offered with the split training set and test set, hence we separate 20% from the training set to form the validation set. Data samples in PhysioNet2012 share the same length, i.e. 48 steps. While samples in PhysioNet2019 have different lengths, hence we only keep samples with lengths larger than 48 and truncate the excess part to ensure samples all have 48 steps as well. For both PhysioNet2012 and PhysioNet2019, samples are firstly split into the training set and the test set according to 80% and 20%, then 20% of samples are taken from the training set as the validation set.

Note that standardization is applied in the preprocessing of all datasets.

B Detailed Description of Models in TSI-Bench

B.1 Transformer-based models

- **iTransformer** [60]: iTransformer repurposes the Transformer architecture by applying attention and feed-forward networks to inverted dimensions, embedding time points into variate tokens to better capture multivariate correlations and nonlinear representations, achieving state-of-the-art performance in time series forecasting.
- **SAITS** [20]: SAITS (Self-Attention-based Imputation for Time Series) is a self-attention imputation transformer with a weighted combination of two diagonally-masked self-attention (DMSA) blocks. It is designed to handle missing data in time series, ensuring robust and accurate data imputation.
- **Nonstationary** [59]: Nonstationary (short for Nonstationary Transformer) addresses the challenge of non-stationarity in time series sequences by incorporating adaptive components that adjust to varying statistical properties over time.
- **ETSformer** [58]: ETSformer integrates exponential smoothing methods with Transformer models, aiming to provide accurate time series forecasting by combining statistical and deep learning approaches.
- **PatchTST** [33]: PatchTST uses a patching strategy combined with a Transformer architecture to enhance the time series forecasting task by capturing both local and global patterns effectively.

⁹<https://physionet.org/content/challenge-2019/1.0.0/>

Table 4: Summary of the 28 benchmarked algorithms, separated by **Architecture**

Model	Category	Architecture	Venue	Year
iTransformer [60]	Forecasting	Transformer	ICLR	2024
SAITS [20]	Imputation	Transformer	ESWA	2023
Nonstationary [59]	Forecasting	Transformer	NeurIPS	2022
ETSformer [58]	Forecasting	Transformer	ArXiv	2022
PatchTST [33]	Forecasting	Transformer	ICLR	2023
Crossformer [43]	Forecasting	Transformer	ICLR	2022
Informer [42]	Forecasting	Transformer	AAAI	2021
Autoformer [31]	Forecasting	Transformer	NeurIPS	2021
Pyraformer [57]	Forecasting	Transformer	ICLR	2021
Transformer [56]	Forecasting	Transformer	NeurIPS	2017
BRITS [19]	Imputation	RNN	NeurIPS	2018
MRNN [61]	Imputation	RNN	TBME	2018
GRUD [62]	Imputation	RNN	Scientific reports	2018
TimesNet [13]	Generic	CNN	ICLR	2023
MICN [63]	Forecasting	CNN	ICLR	2022
SCINet [64]	Forecasting	CNN	NeurIPS	2022
StemGNN [34]	Forecasting	GNN	NeurIPS	2020
FreTS [67]	Forecasting	MLP	NeurIPS	2024
Koopa [66]	Forecasting	MLP	NeurIPS	2024
DLinear [44]	Forecasting	MLP	AAAI	2023
FiLM [65]	Forecasting	MLP	NeurIPS	2022
CSDI [30]	Imputation	Diffusion	NeurIPS	2021
US-GAN [68]	Imputation	GAN	AAAI	2021
GP-VAE [28]	Imputation	VAE	AISTATS	2020
Mean	Imputation	Traditional	-	-
Median	Imputation	Traditional	-	-
LOCF	Imputation	Traditional	-	-
Linear	Imputation	Traditional	-	-

- **Crossformer [43]:** Crossformer leverages cross-dimensional attention to model intricate dependencies within multivariate time series data, achieving good performance in complex forecasting application scenarios.
- **Informer [42]:** Informer enhances efficiency in long time series forecasting by employing a self-attention distillation mechanism, which reduces redundant information while maintaining forecasting accuracy.
- **Autoformer [31]:** Autoformer introduces a novel decomposition architecture with an auto-correlation mechanism, effectively capturing both seasonal and trend patterns in time series forecasting tasks.
- **Pyraformer [57]:** Pyraformer is designed for long-term time series forecasting, utilizing a pyramid attention structure that efficiently captures temporal dependencies at multiple scales.
- **Transformer [71]:** Transformer introduces the self-attention mechanism, which enables the processing of sequential data by attending to different positions within the sequence simultaneously, leading to significant advancements in natural language processing and time series fields.

B.2 RNN-based models

- **BRITS [19]:** BRITS (Bidirectional Recurrent Imputation for Time Series) employs a bidirectional recurrent imputation strategy to handle missing values in time series, improving forecasting accuracy through iterative refinement.
- **MRNN [61]:** The Multi-directional Recurrent Neural Network (MRNN) is designed for estimating missing values in spatiotemporal data and time series by leveraging temporal dependencies and multi-directional information sequence.

- **GRUD [62]:** GRUD (Gated Recurrent Unit for Decay) enhances the Gated Recurrent Unit (GRU) by incorporating decay mechanisms that model the impact of missing values over time, offering robust time series analysis.

B.3 CNN-based models

- **TimesNet [13]:** TimesNet is designed to efficiently model temporal patterns in time series data by incorporating multi-scale temporal convolutions and attention mechanisms. It can be used for short- and long-term forecasting, imputation, classification, and anomaly detection tasks.
- **MICN [63]:** MICN (Multi-scale Inception Convolutional Network) is a convolutional network architecture that captures multi-scale temporal features and combines local and global context for more accurate time series forecasting.
- **SCINet [64]:** SCINet introduces a novel recursive downsample-convolve-interact architecture for time series forecasting, leveraging multiple convolutional filters to extract and aggregate valuable temporal features from downsampled sub-sequences, improving forecasting accuracy over existing models.

B.4 GNN-based models

- **StemGNN [34]:** StemGNN (Spectral Temporal Graph Neural Network) introduces an approach for time series forecasting by jointly capturing inter-series correlations and temporal dependencies in the spectral domain using Graph Fourier Transform (GFT) and Discrete Fourier Transform (DFT), eliminating the need for pre-defined priors.

B.5 MLP-based models

- **FreTS [67]:** FreTS uses MLPs in the frequency domain for time series forecasting, leveraging global view and energy compaction properties to enhance forecasting performance by transforming time-domain signals and learning frequency components.
- **Koopa [66]:** Koopa introduces a novel Koopman forecaster that disentangles time-variant and time-invariant components using Fourier Filter and employs Koopman operators for linear dynamics portrayal, achieving end-to-end forecasting with significant improvements in training time and memory efficiency.
- **DLinear [44]:** DLinear introduces LTSF-Linear, a set of simple one-layer linear models, which outperform complex Transformer-based models in long-term time series forecasting by effectively preserving temporal information that Transformers inherently lose due to their permutation-invariant self-attention mechanism.
- **FiLM [65]:** FiLM (Frequency improved Legendre Memory) introduces a novel approach by using Legendre Polynomials for historical information approximation, Fourier projection for noise reduction, and a low-rank approximation for computational efficiency, resulting in significant improvements in long-term forecasting accuracy.

B.6 Generative models

- **CSDI [30]:** CSDI (Conditional Score-based Diffusion Imputation) leverages conditional score-based diffusion models for accurate imputation and generation of missing values in time series applications.
- **US-GAN [68]:** US-GAN integrates a classifier in a semi-supervised generative adversarial network to enhance its imputation of missing values in multivariate time series, leveraging both observed data and label information. Also, it introduces a temporal matrix to improve the discriminator's ability to differentiate between observed and imputed components.
- **GP-VAE [28]:** GP-VAE (Gaussian Process Variational Autoencoder) proposes a novel deep sequential latent variable model that combines VAE with a structured variational approximation to achieve non-linear dimensionality reduction and imputation, providing interpretable uncertainty estimates and improved imputation smoothness.

B.7 Traditional methods

- **Mean:** The mean imputation method fills in missing values by calculating the mean (average) of the available values in the time series. This method is simple and quick to implement but may not be suitable for data with trends or seasonality, as it does not consider the temporal structure of the data.
- **Median:** Median imputation replaces missing values with the median value of the observed data points. The median is the middle value when the data points are ordered, making this method robust to outliers. It is particularly useful for skewed distributions or data with significant outliers.
- **LOCF:** LOCF (Last Observation Carried Forward) fills in missing values by carrying forward the last observed value. This method assumes that the value remains constant until the next observation is recorded. LOCF is straightforward and works well for short gaps in data, but it can introduce bias if the missing data spans a long period or if the data has a trend.
- **Linear:** Linear interpolation fills in missing values by connecting the last observed value before the missing data and the first observed value after the missing data with a straight line. This method assumes a linear trend between the two points and is useful for data with a relatively stable and linear pattern. However, it may not perform well with data that exhibit non-linear trends or seasonality.

C Details in TSI-Bench

C.1 Missing Patterns

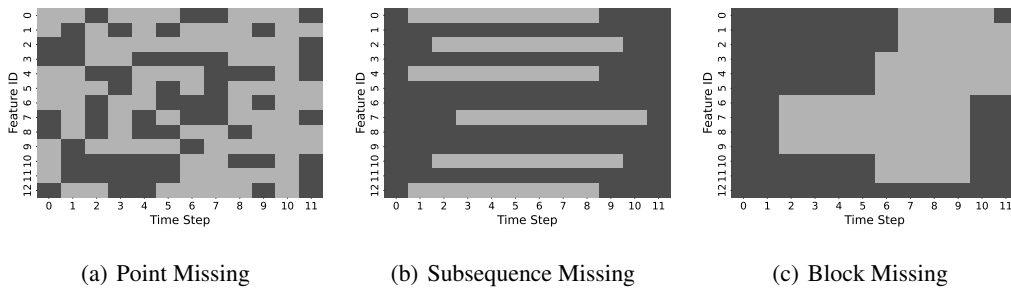


Figure 7: Heatmap visualization of three different missing patterns on the ItalyAir dataset. The observed values are presented in black, while the missing values are in grey.

To explore the imputation algorithms’ performance on different missing patterns, we set up three different modes: point, subsequence, and block. The missingness construction functions are directly available in the Python library PyGrinder¹⁰. The visualization of them is plotted in figures 7(a), 7(b), and 7(c) for vivid illustration.

C.2 Evaluation Metrics

Three metrics are applied to help evaluate the imputation performance in this work: MAE (Mean Absolute Error), MSE (Mean Square Error), and MRE (Mean Relative Error), whose math definitions

¹⁰<https://github.com/WenjieDu/PyGrinder>

are listed below. Note that errors are only calculated for values indicated by the mask in the input.

$$\begin{aligned} \text{MAE}(\hat{y}, y, m) &= \frac{\sum_{d=1}^D \sum_{t=1}^T |(\hat{y}_t^d - y_t^d) \cdot m_t^d|}{\sum_{d=1}^D \sum_{t=1}^T m_t^d} \\ \text{MSE}(\hat{y}, y, m) &= \frac{\sum_{d=1}^D \sum_{t=1}^T ((\hat{y}_t^d - y_t^d) \cdot m_t^d)^2}{\sum_{d=1}^D \sum_{t=1}^T m_t^d} \\ \text{MRE}(\hat{y}, y, m) &= \frac{\sum_{d=1}^D \sum_{t=1}^T |(\hat{y}_t^d - y_t^d) \cdot m_t^d|}{\sum_{d=1}^D \sum_{t=1}^T |y_t^d \cdot m_t^d|} \end{aligned}$$

where \hat{y} is estimated value, y indicates target value, and m means mask with time index t and dimension index d .

C.3 Hyper-parameter Optimization

The performance of deep-learning models highly depends on the settings of hyper-parameters. To make fair comparisons across imputation methods and draw impartial conclusions, all neural network-based algorithms in TSI-Bench get their hyper-parameters optimized by PyPOTS and Microsoft NNI (Neural Network Intelligence). For each algorithm, we run at least 100 trials (i.e. tune it with 100 groups of hyper-parameters) and use the group of the best to produce the formal results. The HPO configuration files and the fixed model hyper-parameters are available in our open-source code repository https://github.com/WenjieDu/Awesome_Imputation.

C.4 Downstream Task Design

To further discuss the benefits that imputation can bring to downstream analysis, experiments are designed and conducted on three common downstream tasks (classification, regression, and forecasting) to evaluate the imputation quality across algorithms. For these three tasks, missing values in the selected datasets are imputed by different algorithms. Then XGBoost, LSTM, and Transformer perform downstream analysis tasks on the imputed datasets with fixed hyper-parameters. XGBoost, LSTM, and Transformer are selected because they are respectively representative models for classical machine learning approaches, traditional RNN methods, and emerging attention algorithms. Besides, thanks to XGBoost it can handle missing values by default. It allows us to compare XGBoost performance results with and without imputation to observe whether imputation can help.

Classification PhysioNet2012 and Pedestrian are chosen for the classification task because their every sample has a classification label. In PhysioNet2012, each sample has a label indicating if the patient is deceased in ICU, making it an unbalanced binary classification dataset with 13.9% positive samples. Sample classes in Pedestrian correspond to ten locations of sensor placement.

Regression ETT_h1 and PeMS both have a target feature that makes them suitable for the regression and forecasting task. In the regression task, except for the target feature, the imputed data with other features are fed into the downstream algorithms to produce the regression results of the target feature.

Forecasting For both ETT_h1 and PeMS datasets, we input the imputed data samples without their target features and the last five steps, then let the downstream models forecast the future five steps of the target feature. Note that, different from the above regression task that inputs the full-length samples and outputs corresponding regression results, the forecasting task holds out the last five steps

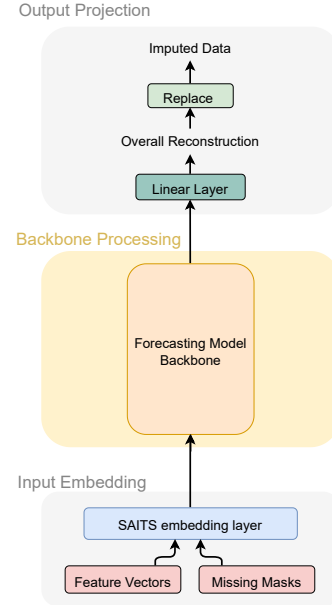


Figure 8: An overview of the adaptation method for forecasting models.

of the samples as ground truth to evaluate the forecasting performance, i.e. its input only contains (sample length - 5) steps.

As additional experiments, the forecasting downstream task is not mentioned in the main body of this paper, but its experimental results are presented in Appendix D.

C.5 Adaptation Paradigm

To tailor the time-series forecasting models for the imputation task, TSI-Bench adopts the imputation framework (including the embedding strategy and the training methodology) from SAITS [20] and proposes such an adaptation paradigm that has been demonstrated to be feasible in this work’s extensive experiments.

Fig. 8 presents an overview of how the forecasting models are transformed to impute missing values in time series. The forecasting model backbone is kept intact, and only the input and output processing are altered to align with the imputation task. In order to well train such a transformed model, the joint-optimization training approach designed for SAITS is employed here, as shown in Fig. 9.

Please refer to the SAITS paper [20] for the details about how this imputation framework works.

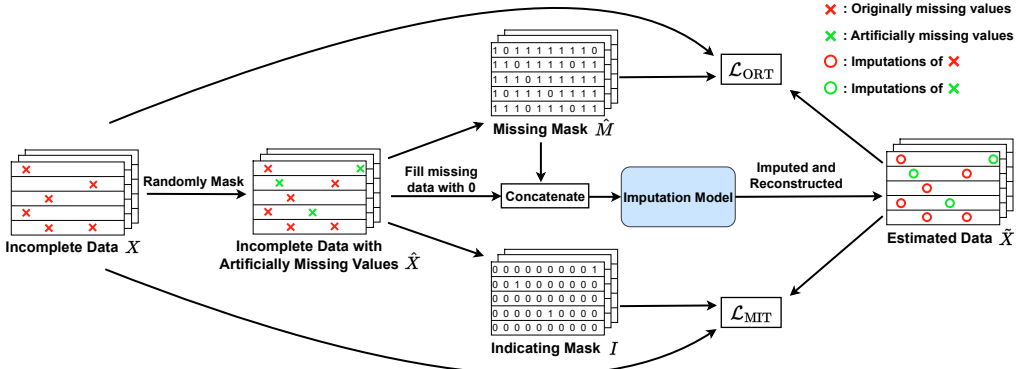


Figure 9: The training methodology from SAITS [20] for the adapted forecasting models.

C.6 Development Environment

All the experiments were conducted on the King’s College London CREATE[72] HPC platform, equipped with 512G RAM and 128 logical cores CPU (AMD EPYC 9554). One NVIDIA A100 80GB GPU is utilized for acceleration for each job, for a total of 32. The software environment is Ubuntu 12.3.0.

To help reproduce our Python environment easily, we freeze the development environment with Anaconda and save it into files for reference, which is publicly available in our GitHub code repository as well.

D Full Experimental Results

In the process of constructing TSI-Bench, to analyze the imputation and downstream task performance of various imputation algorithms on different datasets and obtain valuable insights, we conduct extensive experiments. Specifically, we explore the imputation effects of 28 algorithms under 5 missing patterns and evaluate the performance of downstream tasks after imputation. It should be noted that, as PhysioNet2012 and PhysioNet2019 inherently contain a high proportion of missing data, these two datasets are not included in the experiments with 50% or 90% missing rates.

Note that MICN fails on Pedestrian because the official implementation of its backbone cannot accept univariate time series as input.

Table 5: Details of the preprocessed datasets with 10% point missingness.

Dataset	Air		Traffic		Electricity		Healthcare	
	BeijingAir	ItalyAir	PeMS	Pedestrian	ETTh1	Electricity	PhysioNet2012	PhysioNet2019
# of Total Samples	1458	774	727	3633	358	1457	3997	4927
# of Variables	132	13	862	1	7	370	35	33
Sample Sequence Length	24	12	24	24	48	96	48	48
Time Interval	1H	1H	1H	1H	1H	15Min	1H	1H
Original Missing Rate	1.60%	0%	0%	0%	0%	0%	79.30%	73.90%
Train Missing Rate	11.69%	10.14%	10.01%	9.79%	9.96%	9.99%	80.50%	78.45%
Validation Missing Rate	10.85%	9.77%	9.99%	10.13%	10.24%	10.00%	82.66%	80.30%
Test Missing Rate	11.19%	9.94%	10.04%	9.93%	10.06%	9.99%	82.35%	80.48%
Train Dataset Length	851	466	455	955	212	851	2557	3152
Validation Dataset Length	304	154	122	239	75	304	640	789
Test Dataset Length	303	154	150	2439	71	302	800	986

Table 6: Details of the preprocessed datasets with 50% point missing.

Dataset	Air		Traffic		Electricity	
	BeijingAir	ItalyAir	PeMS	Pedestrian	ETTh1	Electricity
# of Total Samples	1458	774	727	3633	358	1457
# of Variables	132	13	862	1	7	370
Sample Sequence Length	24	12	24	24	48	96
Time Interval	1H	1H	1H	1H	1H	15Min
Original Missing Rate	1.60%	0%	0%	0%	0%	0%
Train Missing Rate	50.98%	50.38%	50.02%	49.60%	50.11%	49.99%
Validation Missing Rate	50.52%	49.70%	50.02%	50.49%	49.49%	50.03%
Test Missing Rate	50.70%	49.96%	50.03%	49.78%	49.97%	49.97%
Train Dataset Length	851	466	455	955	212	851
Validation Dataset Length	304	154	122	239	75	304
Test Dataset Length	303	154	150	2439	71	302

Table 7: Details of the preprocessed datasets with 90% point missing.

Dataset	Air		Traffic		Electricity	
	BeijingAir	ItalyAir	PeMS	Pedestrian	ETTh1	Electricity
# of Total Samples	1458	774	727	3633	358	1457
# of Variables	132	13	862	1	7	370
Sample Sequence Length	24	12	24	24	48	96
Time Interval	1H	1H	1H	1H	1H	15Min
Original Missing Rate	1.60%	0%	0%	0%	0%	0%
Train Missing Rate	90.21%	90.07%	90.00%	90.37%	90.11%	90.00%
Validation Missing Rate	90.12%	89.81%	90.01%	90.17%	89.77%	90.02%
Test Missing Rate	90.21%	89.94%	90.00%	89.74%	90.34%	90.00%
Train Dataset Length	851	466	455	955	212	851
Validation Dataset Length	304	154	122	239	75	304
Test Dataset Length	303	154	150	2439	71	302

Table 8: Details of the preprocessed datasets with 50% subsequence missing.

Dataset	Air		Traffic		Electricity	
	BeijingAir	ItalyAir	PeMS	Pedestrian	ETTh1	Electricity
# of Total Samples	1458	774	727	3633	358	1457
# of Variables	132	13	862	1	7	370
Sample Sequence Length	24	12	24	24	48	96
Time Interval	1H	1H	1H	1H	1H	15Min
Original Missing Rate	1.60%	0%	0%	0%	0%	0%
Train Missing Rate	50.92%	50.01%	50.00%	50.03%	50.03%	50.00%
Validation Missing Rate	50.45%	50.02%	50.00%	50.21%	50.00%	50.00%
Test Missing Rate	50.61%	50.02%	50.00%	50.00%	50.10%	50.00%
Train Dataset Length	851	466	455	955	212	851
Validation Dataset Length	304	154	122	239	75	304
Test Dataset Length	303	154	150	2439	71	302

Table 9: Details of the preprocessed datasets with 50% block missing. The values of Pedestrian are the same as those in Table 8 because this dataset has only 1 feature that makes subsequence missing and block missing identical.

Dataset	Air		Traffic		Electricity	
	BeijingAir	ItalyAir	PeMS	Pedestrian	ETTh1	Electricity
# of Total Samples	1458	774	727	3633	358	1457
# of Variables	132	13	862	1	7	370
Sample Sequence Length	24	12	24	24	48	96
Time Interval	1H	1H	1H	1H	1H	15Min
Original Missing Rate	1.60%	0%	0%	0%	0%	0%
Train Missing Rate	51.19%	50.82%	49.96%	50.03%	49.11%	50.73%
Validation Missing Rate	50.83%	50.97%	50.03%	50.21%	50.42%	50.75%
Test Missing Rate	50.92%	50.28%	50.03%	50.00%	49.58%	50.73%
Train Dataset Length	851	466	455	955	212	851
Validation Dataset Length	304	154	122	239	75	304
Test Dataset Length	303	154	150	2439	71	302

D.1 10% Point Missing

Table 5 shows The details of the datasets involved in the experiments under the 10% missing data setting. Table 10 shows the experimental results of the evaluated methods under the 10% missing data setting, including size, the results of the three evaluation metrics previously mentioned, and inference time.

D.2 50% Point Missing

The details of the datasets involved are shown in Table 6, and Table 11 shows the experimental results of imputation with 50% point missing which is more challenging than with 10% point missing.

D.3 90% Point Missing

The relative details of the datasets are shown in Table 7, and able 12 shows the imputation performance with 90% point missing. This is a relatively extreme scenario and brings difficulties in estimating the missing values.

D.4 50% Subsequence Missing

The details of the preprocessed datasets in this setting is shown as Table 8, and table 13 shows the imputation results with 50% subsequence missing. It could be observed that the imputation error is generally higher than that with 50% point missing. In this condition, the missing values in the subsequence cannot be easily estimated from their adjacent observed data.

D.5 50% Block Missing

Table 9 shows the relative dataset details, and table 14 shows the imputation results under the scenario of 50% block missing. This missing pattern includes missing data across multiple dimensions at the same time points and consecutive missing data at multiple time points, thus presenting challenges for imputation.

D.6 Visualization of Imputation Performance

Figure 10, 11, and 12 depict the imputation examples by different imputation methods. We pick a multivariate time series from the results of each experiment in Appendix D.2, D.4 and D.5 and show imputation results for a single feature of each time series. We can find that most imputation methods can provide reasonable values for the missing components and thus help improve the data quality.

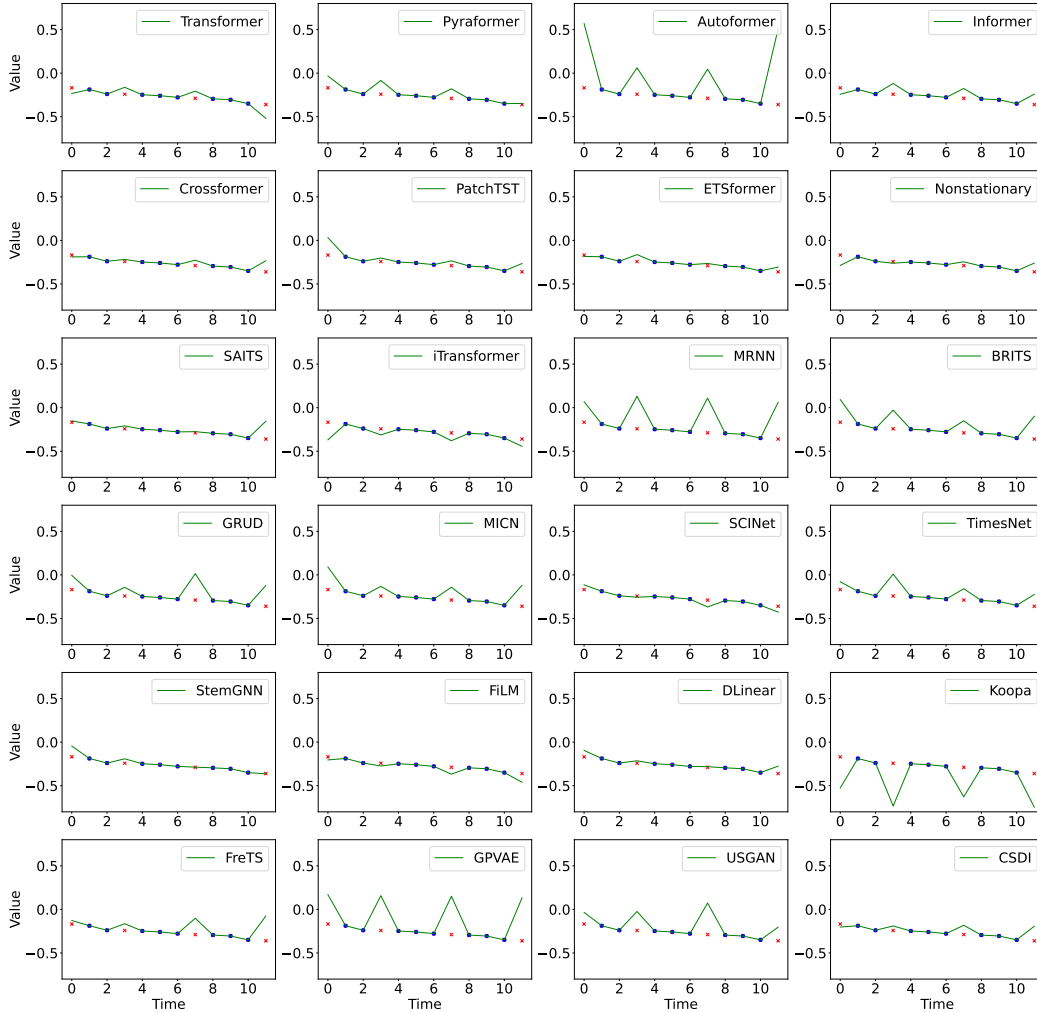


Figure 10: Visualization of imputation performance on the ItalyAir dataset with 50% point missing. Observed values are represented by blue dots, while missing values are indicated with red crosses.

D.7 Experiments on Downstream Tasks

D.7.1 Classification

Table 15 and 16 show the classification performance without and with imputation. In general, the classification performance can be improved after an imputation process for time series with missing values. This observation is particularly evident when using XGBoost as the classification method on the PhysioNet2012 dataset with a missing rate of 10%.

D.7.2 Regression

Table 17, 18 and 19 show the regression performance without and with imputation under 3 different missing patterns. It can be found that when XGBoost is used as the regression model, using advanced algorithms to impute missing values can improve the regression performance overall. However, for some simple methods (such as Mean), the regression effect after imputation may not improve or may become worse, which also shows to some extent that it is meaningful and valuable to research on the missing value imputation in time series.

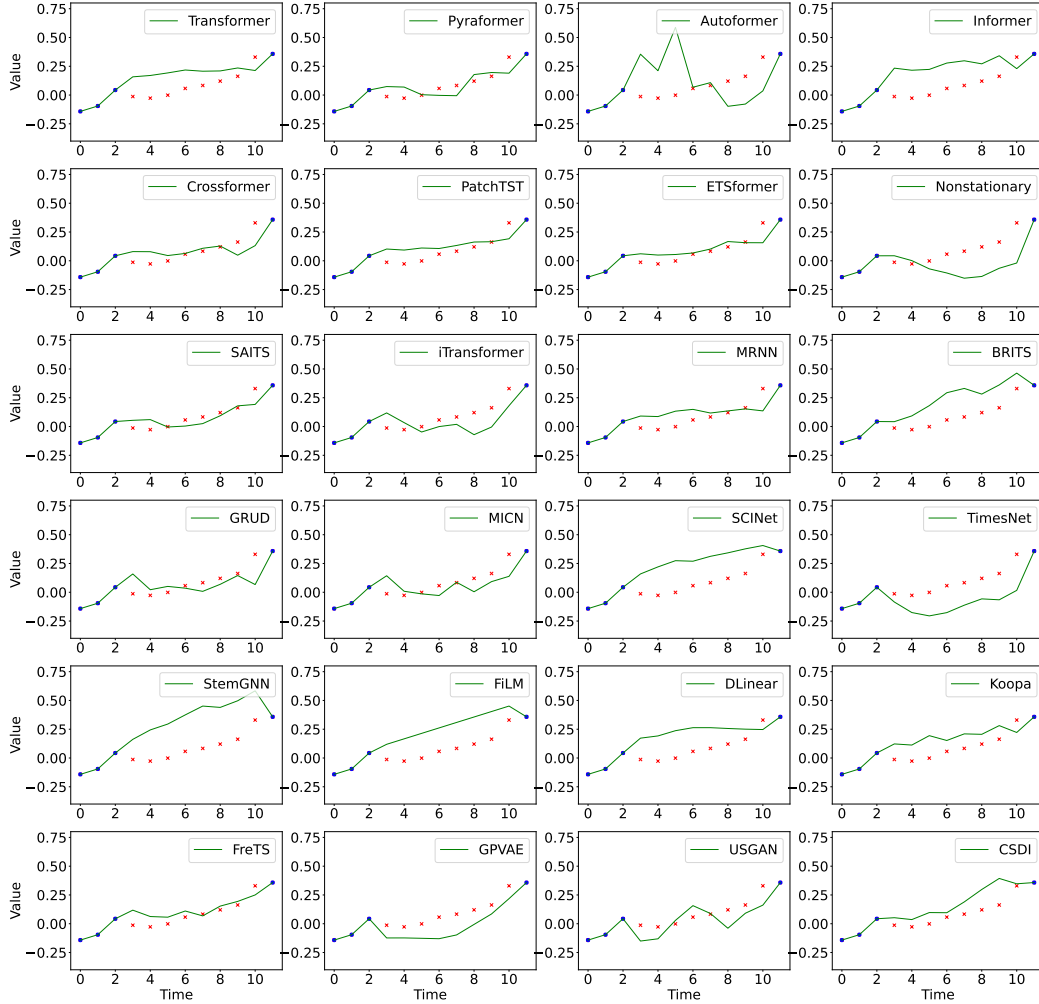


Figure 11: Visualization of imputation performance on the ItalyAir dataset with 50% subsequence missing. Observed values are represented by blue dots, while missing values are indicated with red crosses.

D.7.3 Forecasting

Table 20, 21 and 22 show the forecasting performance without or with imputation under different missing patterns and show the same phenomenon when regression is the downstream task, that is, using advanced algorithms to impute missing values can improve the performance of downstream tasks, while using simple methods like Mean may not have a positive impact on forecasting performance.

D.8 The total number of experiments

We conduct a total of 34,804 experiments across 28 algorithms and 8 datasets, focusing on 3 angles (i.e., on the data level, the model level, and the downstream tasks) for a comprehensive and fair evaluation and analysis through the experiments. Note that duplicated experiments for obtaining the final stable results are not included here.

HPO experiments. For 24 neural networks, we run 100 HPO trials for each of them on each dataset, $24 * 100 * 8 = 19,200$

Imputation experiments. For 24 neural network models, we run 5 rounds on 8 datasets with 10% point missing, 6 datasets with 50% point missing, 6 datasets with 90% point missing, 6 datasets

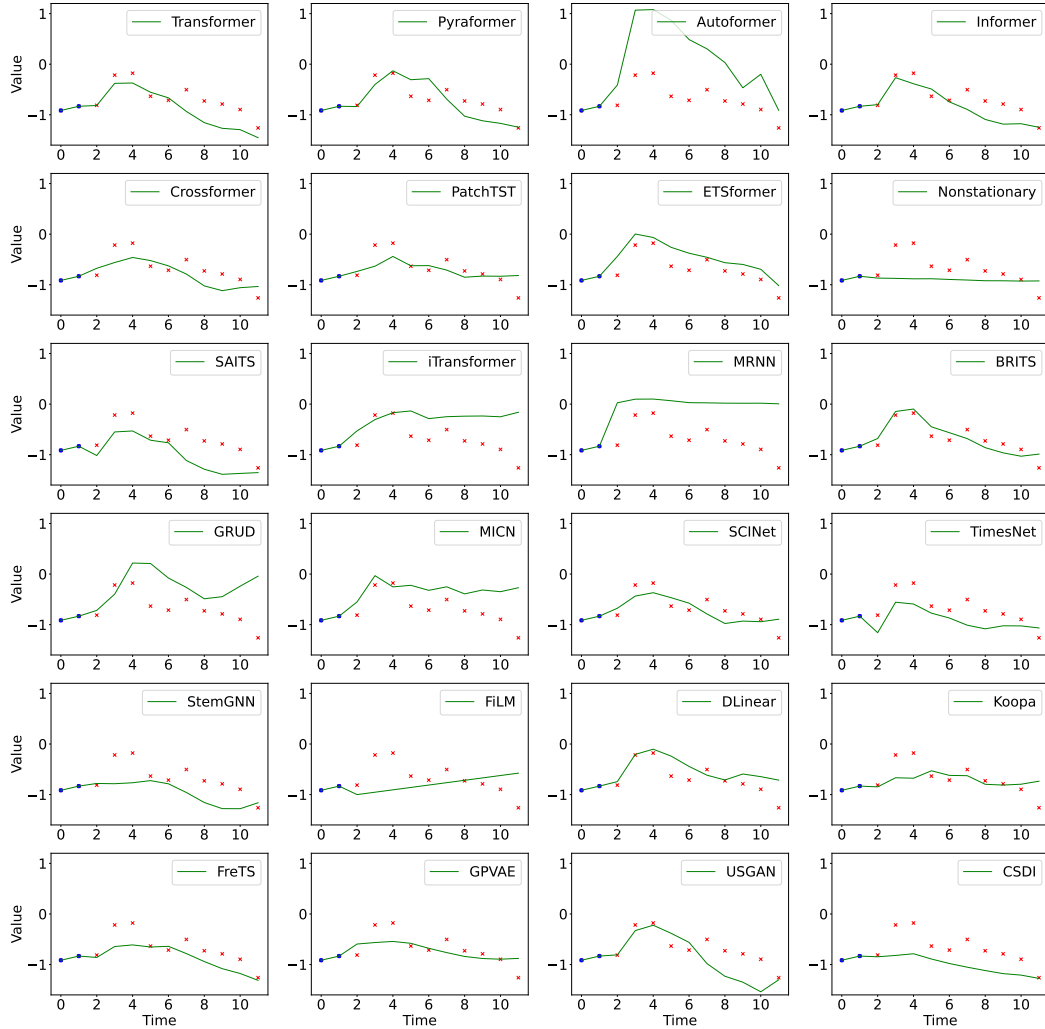


Figure 12: Visualization of imputation performance on the ItalyAir dataset with 50% block missing. Observed values are represented by blue dots, while missing values are indicated with red crosses.

with 50% subsequence missing, and 5 datasets with 50% block missing: $24 \cdot 5 \cdot (8+6+6+6+5) = 3,720$. $4 \cdot (8+6+6+6+5) = 124$ for 4 naive imputation methods.

Downstream experiments. Experiments on the downstream tasks are performed 5 rounds with 4 algorithms on each dataset imputed by 28 methods. The classification task is on PhysioNet2012 with 10% point missing in the evaluation sets and Pedestrian with 10%, 50%, and 90% point missing, and 50% subsequence missing. The regression and forecasting tasks are on ETT_h1 and PeMS with 10% and 50% point missing, 50% subsequence missing and block missing. $5 \cdot 4 \cdot 28 \cdot (1+4) + 5 \cdot 4 \cdot 28 \cdot (4+4) + 5 \cdot 4 \cdot 28 \cdot (4+4) = 11,760$

Table 15: Performance comparison for the classification task on PhysioNet2012 and Pedestrian datasets with 10% point missing.

PhysioNet2012 (10% missing rate)									
	PR_AUC wt XGB	PR_AUC w XGB	PR_AUC w RNN	PR_AUC w Transformer	ROC_AUC wt XGB	ROC_AUC w XGB	ROC_AUC w RNN	ROC_AUC w Transformer	
iTransformer	0.521 (0.000)	0.359 (0.049)	0.286 (0.040)	0.277 (0.039)	0.852 (0.000)	0.692 (0.073)	0.685 (0.032)	0.685 (0.032)	
SAITS	0.490 (0.000)	0.274 (0.054)	0.277 (0.039)	0.374 (0.061)	0.851 (0.000)	0.658 (0.076)	0.668 (0.037)	0.668 (0.037)	
Nonstationary	0.542 (0.000)	0.294 (0.029)	0.374 (0.061)	0.278 (0.013)	0.860 (0.000)	0.583 (0.078)	0.721 (0.049)	0.721 (0.049)	
ETSformer	0.433 (0.000)	0.392 (0.035)	0.278 (0.013)	0.303 (0.067)	0.820 (0.000)	0.734 (0.030)	0.678 (0.013)	0.678 (0.013)	
PatchTST	0.512 (0.000)	0.347 (0.038)	0.303 (0.067)	0.253 (0.032)	0.848 (0.000)	0.703 (0.064)	0.698 (0.061)	0.698 (0.061)	
Crossformer	0.489 (0.000)	0.317 (0.029)	0.253 (0.032)	0.283 (0.046)	0.836 (0.000)	0.683 (0.051)	0.644 (0.026)	0.644 (0.026)	
Informr	0.468 (0.000)	0.306 (0.046)	0.283 (0.046)	0.223 (0.009)	0.836 (0.000)	0.701 (0.021)	0.653 (0.029)	0.653 (0.029)	
Autoformer	0.368 (0.000)	0.203 (0.008)	0.223 (0.009)	0.250 (0.047)	0.768 (0.000)	0.597 (0.009)	0.625 (0.008)	0.625 (0.008)	
Pyraformer	0.461 (0.000)	0.381 (0.017)	0.250 (0.047)	0.250 (0.047)	0.829 (0.000)	0.739 (0.026)	0.654 (0.047)	0.654 (0.047)	
Transformer	0.458 (0.000)	0.360 (0.034)	0.250 (0.047)	0.223 (0.024)	0.833 (0.000)	0.723 (0.036)	0.626 (0.036)	0.626 (0.036)	
BRITS	0.455 (0.000)	0.315 (0.069)	0.270 (0.068)	0.270 (0.068)	0.841 (0.000)	0.667 (0.066)	0.646 (0.074)	0.646 (0.074)	
MRNN	0.346 (0.000)	0.232 (0.013)	0.219 (0.012)	0.219 (0.012)	0.760 (0.000)	0.611 (0.008)	0.619 (0.015)	0.619 (0.015)	
GRU	0.423 (0.000)	0.373 (0.064)	0.392 (0.058)	0.392 (0.058)	0.840 (0.000)	0.721 (0.075)	0.745 (0.035)	0.745 (0.035)	
TimesNet	0.432 (0.000)	0.332 (0.055)	0.344 (0.062)	0.344 (0.062)	0.823 (0.000)	0.687 (0.087)	0.710 (0.043)	0.710 (0.043)	
MICN	0.410 (0.000)	0.316 (0.069)	0.295 (0.058)	0.295 (0.058)	0.824 (0.000)	0.700 (0.071)	0.686 (0.050)	0.686 (0.050)	
SCINet	0.388 (0.000)	0.319 (0.071)	0.340 (0.052)	0.340 (0.052)	0.771 (0.000)	0.663 (0.055)	0.720 (0.034)	0.720 (0.034)	
StemGNN	0.423 (0.000)	0.277 (0.074)	0.312 (0.024)	0.312 (0.024)	0.809 (0.000)	0.534 (0.124)	0.701 (0.025)	0.701 (0.025)	
FreTS	0.471 (0.000)	0.333 (0.025)	0.275 (0.012)	0.275 (0.012)	0.840 (0.000)	0.693 (0.035)	0.674 (0.018)	0.674 (0.018)	
Koopaa	0.470 (0.000)	0.237 (0.056)	0.238 (0.039)	0.238 (0.039)	0.835 (0.000)	0.509 (0.113)	0.628 (0.036)	0.628 (0.036)	
DLlinear	0.486 (0.000)	0.323 (0.057)	0.230 (0.034)	0.230 (0.034)	0.851 (0.000)	0.689 (0.038)	0.611 (0.053)	0.611 (0.053)	
FILM	0.422 (0.000)	0.292 (0.058)	0.361 (0.066)	0.361 (0.066)	0.825 (0.000)	0.565 (0.095)	0.706 (0.046)	0.706 (0.046)	
CSDI	0.459 (0.000)	0.291 (0.056)	0.438 (0.016)	0.438 (0.016)	0.853 (0.000)	0.553 (0.108)	0.762 (0.019)	0.762 (0.019)	
US-GAN	0.492 (0.000)	0.333 (0.044)	0.223 (0.046)	0.223 (0.046)	0.839 (0.000)	0.708 (0.019)	0.610 (0.043)	0.610 (0.043)	
GP-VAE	0.456 (0.000)	0.396 (0.036)	0.334 (0.072)	0.334 (0.072)	0.816 (0.000)	0.745 (0.056)	0.701 (0.041)	0.701 (0.041)	
Mean	0.384 (0.000)	0.251 (0.022)	0.200 (0.016)	0.200 (0.016)	0.763 (0.000)	0.620 (0.017)	0.598 (0.025)	0.598 (0.025)	
Median	0.361 (0.023)	0.236 (0.024)	0.206 (0.015)	0.206 (0.015)	0.772 (0.010)	0.619 (0.013)	0.605 (0.025)	0.605 (0.025)	
LOCF	0.391 (0.045)	0.267 (0.073)	0.277 (0.102)	0.277 (0.102)	0.795 (0.033)	0.634 (0.074)	0.644 (0.061)	0.644 (0.061)	
Linear	0.417 (0.060)	0.289 (0.078)	0.309 (0.111)	0.309 (0.111)	0.807 (0.036)	0.640 (0.076)	0.669 (0.069)	0.669 (0.069)	
Pedestrian (10% missing rate)									
	PR_AUC wt XGB	PR_AUC w XGB	PR_AUC w RNN	PR_AUC w Transformer	ROC_AUC wt XGB	ROC_AUC w XGB	ROC_AUC w RNN	ROC_AUC w Transformer	
iTransformer	0.977 (0.000)	0.478 (0.079)	0.903 (0.011)	0.903 (0.011)	0.996 (0.000)	0.896 (0.026)	0.985 (0.001)	0.985 (0.001)	
SAITS	0.982 (0.000)	0.458 (0.050)	0.926 (0.024)	0.926 (0.024)	0.997 (0.000)	0.890 (0.020)	0.989 (0.003)	0.989 (0.003)	
Nonstationary	0.973 (0.000)	0.485 (0.060)	0.956 (0.000)	0.956 (0.000)	0.996 (0.000)	0.902 (0.020)	0.993 (0.000)	0.993 (0.000)	
ETSformer	0.977 (0.000)	0.487 (0.057)	0.910 (0.035)	0.910 (0.035)	0.996 (0.000)	0.901 (0.020)	0.986 (0.005)	0.986 (0.005)	
PatchTST	0.981 (0.000)	0.463 (0.058)	0.915 (0.029)	0.915 (0.029)	0.997 (0.000)	0.892 (0.019)	0.988 (0.004)	0.988 (0.004)	
Crossformer	0.980 (0.000)	0.509 (0.054)	0.923 (0.036)	0.923 (0.036)	0.997 (0.000)	0.907 (0.016)	0.989 (0.005)	0.989 (0.005)	
Informr	0.980 (0.000)	0.479 (0.049)	0.908 (0.026)	0.908 (0.026)	0.997 (0.000)	0.898 (0.015)	0.986 (0.004)	0.986 (0.004)	
Autoformer	0.978 (0.000)	0.480 (0.086)	0.932 (0.027)	0.932 (0.027)	0.996 (0.000)	0.898 (0.025)	0.989 (0.004)	0.989 (0.004)	
Pyraformer	0.978 (0.000)	0.506 (0.064)	0.939 (0.022)	0.939 (0.022)	0.997 (0.000)	0.908 (0.018)	0.991 (0.003)	0.991 (0.003)	
Transformer	0.979 (0.000)	0.496 (0.051)	0.897 (0.019)	0.897 (0.019)	0.997 (0.000)	0.902 (0.015)	0.985 (0.003)	0.985 (0.003)	
BRITS	0.981 (0.000)	0.462 (0.051)	0.938 (0.027)	0.938 (0.027)	0.997 (0.000)	0.898 (0.017)	0.991 (0.004)	0.991 (0.004)	
MRNN	0.970 (0.000)	0.474 (0.051)	0.916 (0.011)	0.916 (0.011)	0.995 (0.000)	0.900 (0.017)	0.987 (0.002)	0.987 (0.002)	
GRU	0.977 (0.000)	0.493 (0.058)	0.916 (0.025)	0.916 (0.025)	0.997 (0.000)	0.899 (0.019)	0.988 (0.003)	0.988 (0.003)	
TimesNet	0.978 (0.000)	0.503 (0.064)	0.910 (0.034)	0.910 (0.034)	0.997 (0.000)	0.906 (0.021)	0.987 (0.005)	0.987 (0.005)	
MICN	0.972 (0.000)	0.502 (0.051)	0.902 (0.022)	0.902 (0.022)	0.996 (0.000)	0.904 (0.017)	0.986 (0.003)	0.986 (0.003)	
SCINet	0.981 (0.000)	0.483 (0.034)	0.928 (0.038)	0.928 (0.038)	0.997 (0.000)	0.899 (0.009)	0.989 (0.005)	0.989 (0.005)	
StemGNN	0.982 (0.000)	0.474 (0.063)	0.902 (0.028)	0.902 (0.028)	0.997 (0.000)	0.895 (0.023)	0.985 (0.004)	0.985 (0.004)	
FreTS	0.978 (0.000)	0.498 (0.047)	0.907 (0.050)	0.907 (0.050)	0.997 (0.000)	0.906 (0.014)	0.986 (0.006)	0.986 (0.006)	
Koopaa	0.981 (0.000)	0.520 (0.054)	0.904 (0.029)	0.904 (0.029)	0.997 (0.000)	0.912 (0.016)	0.986 (0.004)	0.986 (0.004)	
DLlinear	0.973 (0.000)	0.482 (0.020)	0.955 (0.007)	0.955 (0.007)	0.996 (0.000)	0.903 (0.007)	0.992 (0.001)	0.992 (0.001)	
FILM	0.978 (0.000)	0.511 (0.048)	0.924 (0.029)	0.924 (0.029)	0.996 (0.000)	0.907 (0.019)	0.989 (0.004)	0.989 (0.004)	
CSDI	0.979 (0.000)	0.498 (0.045)	0.941 (0.011)	0.941 (0.011)	0.997 (0.000)	0.905 (0.014)	0.991 (0.002)	0.991 (0.002)	
US-GAN	0.974 (0.000)	0.472 (0.065)	0.898 (0.003)	0.898 (0.003)	0.996 (0.000)	0.893 (0.020)	0.985 (0.001)	0.985 (0.001)	
GP-VAE	0.970 (0.000)	0.486 (0.050)	0.912 (0.018)	0.912 (0.018)	0.995 (0.000)	0.904 (0.019)	0.986 (0.003)	0.986 (0.003)	
Mean	0.968 (0.002)	0.498 (0.068)	0.900 (0.019)	0.900 (0.019)	0.996 (0.000)	0.906 (0.023)	0.984 (0.003)	0.984 (0.003)	
Median	0.971 (0.004)	0.489 (0.063)	0.909 (0.023)	0.909 (0.023)	0.996 (0.000)	0.903 (0.021)	0.986 (0.004)	0.986 (0.004)	
LOCF	0.973 (0.005)	0.498 (0.059)	0.916 (0.025)	0.916 (0.025)	0.996 (0.001)	0.906 (0.019)	0.987 (0.004)	0.987 (0.004)	
Linear									

Table 16: Performance comparison for the classification task on Pedestrian datasets with 50% point missing, 90% point missing, and 50% subsequence missing.

	Pedestrian (50% point missing rate)					
	PR_AUC wt XGB	PR_AUC w XGB	PR_AUC w RNN	PR_AUC w Transformer	ROC_AUC wt XGB	ROC_AUC w Transformer
Transformer	0.936 (0.000)	0.945 (0.010)	0.848 (0.011)	0.848 (0.011)	0.990 (0.000)	0.901 (0.022)
Nonstationary	0.906 (0.000)	0.866 (0.007)	0.865 (0.016)	0.865 (0.016)	0.984 (0.000)	0.972 (0.003)
ETSformer	0.900 (0.000)	0.286 (0.097)	0.805 (0.016)	0.805 (0.016)	0.990 (0.000)	0.968 (0.002)
PatchST	0.948 (0.000)	0.563 (0.038)	0.782 (0.034)	0.782 (0.034)	0.925 (0.010)	0.964 (0.006)
Crossformer	0.942 (0.000)	0.518 (0.080)	0.839 (0.010)	0.839 (0.010)	0.994 (0.002)	0.974 (0.001)
Autoformer	0.952 (0.000)	0.850 (0.021)	0.850 (0.021)	0.850 (0.021)	0.991 (0.000)	0.975 (0.003)
Pyraformer	0.941 (0.000)	0.828 (0.024)	0.828 (0.024)	0.828 (0.024)	0.991 (0.000)	0.975 (0.003)
Transformer	0.951 (0.000)	0.483 (0.059)	0.850 (0.021)	0.850 (0.021)	0.991 (0.000)	0.973 (0.004)
BRITS	0.929 (0.000)	0.470 (0.073)	0.846 (0.015)	0.846 (0.015)	0.989 (0.000)	0.971 (0.003)
MRNN	0.884 (0.000)	0.479 (0.130)	0.694 (0.018)	0.694 (0.018)	0.981 (0.000)	0.945 (0.003)
GRU	0.932 (0.000)	0.579 (0.030)	0.817 (0.017)	0.817 (0.017)	0.989 (0.000)	0.969 (0.003)
TimesNet	0.912 (0.000)	0.460 (0.038)	0.835 (0.011)	0.835 (0.011)	0.983 (0.000)	0.970 (0.003)
MICN					0.986 (0.000)	
SCINet	0.924 (0.000)	0.497 (0.064)	0.856 (0.008)	0.856 (0.008)	0.988 (0.000)	0.902 (0.021)
StemGNN	0.943 (0.000)	0.495 (0.025)	0.854 (0.005)	0.854 (0.005)	0.991 (0.000)	0.975 (0.002)
FreTS	0.935 (0.000)	0.474 (0.079)	0.829 (0.020)	0.829 (0.020)	0.990 (0.000)	0.976 (0.004)
Koopa	0.918 (0.000)	0.491 (0.069)	0.859 (0.011)	0.859 (0.011)	0.987 (0.000)	0.972 (0.004)
DLear	0.882 (0.000)	0.530 (0.025)	0.798 (0.016)	0.798 (0.016)	0.981 (0.000)	0.975 (0.002)
FLIM	0.894 (0.000)	0.545 (0.048)	0.772 (0.019)	0.772 (0.019)	0.983 (0.000)	0.961 (0.003)
SDI	0.921 (0.000)	0.449 (0.029)	0.857 (0.007)	0.857 (0.007)	0.987 (0.000)	0.975 (0.002)
US-GAN	0.925 (0.000)	0.565 (0.020)	0.872 (0.007)	0.872 (0.007)	0.989 (0.000)	0.975 (0.002)
GP-VAE	0.877 (0.000)	0.565 (0.020)	0.726 (0.021)	0.726 (0.021)	0.989 (0.000)	0.955 (0.003)
Mean	0.884 (0.000)	0.500 (0.035)	0.492 (0.045)	0.492 (0.045)	0.981 (0.000)	0.944 (0.003)
Median	0.881 (0.004)	0.481 (0.089)	0.717 (0.029)	0.717 (0.029)	0.981 (0.000)	0.948 (0.005)
LOCF	0.895 (0.020)	0.511 (0.086)	0.750 (0.052)	0.750 (0.052)	0.983 (0.003)	0.906 (0.042)
Linear	0.904 (0.024)	0.525 (0.081)	0.768 (0.056)	0.768 (0.056)	0.984 (0.004)	0.911 (0.038)
Pedestrian (90% point missing rate)						
PR_AUC wt XGB	PR_AUC w XGB	PR_AUC w RNN	PR_AUC w Transformer	ROC_AUC wt XGB	ROC_AUC w RNN	ROC_AUC w Transformer
Transformer	0.332 (0.000)	0.254 (0.069)	0.332 (0.005)	0.332 (0.005)	0.845 (0.000)	0.784 (0.020)
Nonstationary	0.386 (0.000)	0.242 (0.027)	0.348 (0.011)	0.348 (0.011)	0.843 (0.000)	0.826 (0.003)
ETSformer	0.329 (0.000)	0.179 (0.016)	0.310 (0.019)	0.310 (0.019)	0.828 (0.000)	0.659 (0.046)
PatchST	0.339 (0.000)	0.232 (0.013)	0.340 (0.017)	0.340 (0.017)	0.809 (0.000)	0.756 (0.024)
Crossformer	0.391 (0.000)	0.197 (0.029)	0.383 (0.020)	0.383 (0.020)	0.846 (0.000)	0.680 (0.065)
Autoformer	0.389 (0.000)	0.258 (0.013)	0.387 (0.006)	0.387 (0.006)	0.833 (0.000)	0.855 (0.002)
Pyraformer	0.327 (0.000)	0.244 (0.007)	0.265 (0.005)	0.265 (0.005)	0.801 (0.000)	0.760 (0.007)
Transformer	0.405 (0.000)	0.266 (0.009)	0.349 (0.021)	0.349 (0.021)	0.847 (0.000)	0.784 (0.022)
BRITS	0.400 (0.000)	0.237 (0.046)	0.347 (0.019)	0.347 (0.019)	0.842 (0.000)	0.710 (0.092)
MRNN	0.406 (0.000)	0.259 (0.011)	0.371 (0.019)	0.371 (0.019)	0.848 (0.000)	0.786 (0.009)
GRU	0.434 (0.000)	0.259 (0.007)	0.339 (0.016)	0.339 (0.016)	0.841 (0.000)	0.778 (0.006)
TimesNet	0.433 (0.000)	0.312 (0.005)	0.351 (0.009)	0.351 (0.009)	0.859 (0.000)	0.839 (0.002)
SCINet	0.330 (0.000)	0.244 (0.006)	0.324 (0.018)	0.324 (0.018)	0.811 (0.000)	0.776 (0.004)
StemGNN	0.380 (0.000)	0.210 (0.052)	0.326 (0.011)	0.326 (0.011)	0.841 (0.000)	0.687 (0.111)
FreTS	0.394 (0.000)	0.195 (0.018)	0.357 (0.020)	0.357 (0.020)	0.846 (0.000)	0.693 (0.052)
Koopa	0.396 (0.000)	0.226 (0.024)	0.367 (0.010)	0.367 (0.010)	0.848 (0.000)	0.717 (0.076)
DLear	0.376 (0.000)	0.238 (0.032)	0.383 (0.013)	0.383 (0.013)	0.836 (0.000)	0.753 (0.026)
FLIM	0.335 (0.000)	0.235 (0.009)	0.335 (0.011)	0.335 (0.011)	0.844 (0.000)	0.694 (0.046)
FLIM	0.333 (0.000)	0.237 (0.006)	0.318 (0.018)	0.318 (0.018)	0.818 (0.000)	0.922 (0.048)
CSN	0.350 (0.000)	0.252 (0.025)	0.345 (0.017)	0.345 (0.017)	0.790 (0.000)	0.773 (0.068)
US-GAN	0.382 (0.000)	0.240 (0.038)	0.369 (0.017)	0.369 (0.017)	0.845 (0.000)	0.748 (0.085)
GP-VAE	0.420 (0.000)	0.237 (0.018)	0.300 (0.033)	0.300 (0.033)	0.847 (0.000)	0.749 (0.023)
Mean	0.413 (0.000)	0.217 (0.009)	0.291 (0.033)	0.291 (0.033)	0.830 (0.000)	0.728 (0.012)
Median	0.414 (0.002)	0.217 (0.007)	0.288 (0.029)	0.288 (0.029)	0.830 (0.000)	0.728 (0.009)
LOCF	0.432 (0.025)	0.246 (0.041)	0.303 (0.033)	0.303 (0.033)	0.841 (0.016)	0.758 (0.042)
Linear	0.425 (0.025)	0.255 (0.039)	0.310 (0.032)	0.310 (0.032)	0.841 (0.014)	0.769 (0.041)
Pedestrian (50% subsequence missing rate)						
PR_AUC wt XGB	PR_AUC w XGB	PR_AUC w RNN	PR_AUC w Transformer	ROC_AUC wt XGB	ROC_AUC w RNN	ROC_AUC w Transformer
Transformer	0.750 (0.000)	0.201 (0.034)	0.553 (0.007)	0.553 (0.007)	0.932 (0.000)	0.676 (0.053)
Nonstationary	0.729 (0.000)	0.251 (0.086)	0.584 (0.024)	0.584 (0.024)	0.955 (0.000)	0.927 (0.004)
ETSformer	0.743 (0.000)	0.217 (0.037)	0.499 (0.011)	0.499 (0.011)	0.946 (0.000)	0.712 (0.131)
PatchST	0.743 (0.000)	0.223 (0.043)	0.544 (0.022)	0.544 (0.022)	0.950 (0.000)	0.733 (0.054)
Crossformer	0.747 (0.000)	0.215 (0.038)	0.532 (0.022)	0.532 (0.022)	0.952 (0.000)	0.715 (0.060)
Autoformer	0.745 (0.000)	0.236 (0.039)	0.557 (0.030)	0.557 (0.030)	0.952 (0.000)	0.652 (0.099)
Pyraformer	0.755 (0.000)	0.203 (0.094)	0.562 (0.013)	0.562 (0.013)	0.953 (0.000)	0.737 (0.050)
Transformer	0.741 (0.000)	0.238 (0.067)	0.582 (0.028)	0.582 (0.028)	0.953 (0.000)	0.627 (0.198)
BRITS	0.762 (0.000)	0.255 (0.033)	0.519 (0.037)	0.519 (0.037)	0.954 (0.000)	0.721 (0.079)
MRNN	0.758 (0.000)	0.183 (0.035)	0.574 (0.018)	0.574 (0.018)	0.952 (0.000)	0.627 (0.077)
GRU	0.733 (0.000)	0.232 (0.075)	0.485 (0.033)	0.485 (0.033)	0.947 (0.000)	0.694 (0.115)
TimesNet	0.753 (0.000)	0.271 (0.082)	0.538 (0.021)	0.538 (0.021)	0.949 (0.000)	0.756 (0.089)
SCINet	0.760 (0.000)	0.305 (0.072)	0.555 (0.025)	0.555 (0.025)	0.954 (0.000)	0.808 (0.059)
StemGNN	0.741 (0.000)	0.211 (0.040)	0.584 (0.040)	0.584 (0.040)	0.932 (0.000)	0.658 (0.098)
FreTS	0.743 (0.000)	0.259 (0.052)	0.565 (0.019)	0.565 (0.019)	0.950 (0.000)	0.751 (0.087)
Koopa	0.752 (0.000)	0.180 (0.027)	0.539 (0.024)	0.539 (0.024)	0.953 (0.000)	0.823 (0.053)
DLear	0.743 (0.000)	0.212 (0.052)	0.572 (0.030)	0.572 (0.030)	0.951 (0.000)	0.686 (0.107)
FLIM	0.730 (0.000)	0.246 (0.039)	0.530 (0.027)	0.530 (0.027)	0.948 (0.000)	0.815 (0.037)
CSN	0.732 (0.000)	0.273 (0.083)	0.573 (0.083)	0.573 (0.083)	0.948 (0.000)	0.756 (0.091)
US-GAN	0.743 (0.000)	0.295 (0.091)	0.530 (0.025)	0.530 (0.025)	0.950 (0.000)	0.783 (0.103)
GP-VAE	0.734 (0.000)	0.258 (0.034)	0.534 (0.019)	0.534 (0.019)	0.948 (0.000)	0.779 (0.040)
Mean	0.724 (0.000)	0.215 (0.099)	0.475 (0.019)	0.475 (0.019)	0.945 (0.000)	0.642 (0.167)
Median	0.714 (0.010)	0.198 (0.076)	0.472 (0.023)	0.472 (0.023)	0.944 (0.002)	0.622 (0.142)
LOCF	0.717 (0.009)	0.209 (0.069)	0.474 (0.026)	0.474 (0.026)	0.944 (0.002)	0.664 (0.137)
Linear	0.727 (0.019)	0.225 (0.070)	0.487 (0.034)	0.487 (0.034)	0.946 (0.004)	0.696 (0.133)

Table 18: Performance comparison for the regression task on ETT_h1 datasets with 10% point missing and 50% point missing.

	ETT_h1 (point_10%)									
	MAE w/ XGB	MRE w/ XGB	MSE w/ XGB	MAE w/ XGB	MRE w/ XGB	MSE w/ XGB	MSE w/ RNN	MRE w/ RNN	MSE w/ Transformer	MRE w/ Transformer
Transformer	1.194 (0.000)	1.054 (0.000)	1.773 (0.000)	1.403 (0.057)	1.239 (0.051)	2.352 (0.139)	1.401 (0.071)	1.237 (0.065)	2.260 (0.187)	
SAlTS	1.186 (0.000)	1.047 (0.000)	1.708 (0.000)	1.403 (0.058)	1.239 (0.051)	2.352 (0.141)	1.397 (0.073)	1.233 (0.065)	2.248 (0.193)	
Nonstationary	1.161 (0.000)	1.025 (0.000)	1.664 (0.000)	1.424 (0.057)	1.258 (0.050)	2.417 (0.138)	1.399 (0.075)	1.236 (0.066)	2.260 (0.198)	
ETStformer	1.151 (0.000)	1.016 (0.000)	1.617 (0.000)	1.400 (0.057)	1.236 (0.050)	2.344 (0.138)	1.393 (0.070)	1.230 (0.062)	2.238 (0.182)	
PatchTST	1.166 (0.000)	1.029 (0.000)	1.672 (0.000)	1.406 (0.056)	1.242 (0.049)	2.360 (0.136)	1.390 (0.073)	1.228 (0.065)	2.229 (0.191)	
Crossformer	1.152 (0.000)	1.018 (0.000)	1.637 (0.000)	1.403 (0.056)	1.239 (0.050)	2.351 (0.137)	1.393 (0.072)	1.230 (0.064)	2.239 (0.187)	
Informor	1.155 (0.000)	1.020 (0.000)	1.648 (0.000)	1.401 (0.057)	1.238 (0.051)	2.347 (0.139)	1.399 (0.073)	1.235 (0.065)	2.253 (0.192)	
Autoformer	1.159 (0.000)	1.023 (0.000)	1.636 (0.000)	1.401 (0.057)	1.237 (0.050)	2.344 (0.137)	1.390 (0.072)	1.228 (0.062)	2.228 (0.184)	
Pyraformer	1.166 (0.000)	1.030 (0.000)	1.672 (0.000)	1.404 (0.056)	1.239 (0.050)	2.353 (0.137)	1.397 (0.071)	1.233 (0.064)	2.247 (0.189)	
Transformer	1.144 (0.000)	1.010 (0.000)	1.589 (0.000)	1.401 (0.057)	1.237 (0.050)	2.346 (0.138)	1.395 (0.073)	1.232 (0.065)	2.241 (0.192)	
BRITS	1.147 (0.000)	1.012 (0.000)	1.574 (0.000)	1.401 (0.057)	1.237 (0.051)	2.346 (0.139)	1.394 (0.073)	1.231 (0.065)	2.240 (0.192)	
MRNN	1.157 (0.000)	1.022 (0.000)	1.639 (0.000)	1.374 (0.062)	1.213 (0.055)	2.268 (0.151)	1.387 (0.078)	1.225 (0.069)	2.221 (0.208)	
GRU4Rec	1.172 (0.000)	1.035 (0.000)	1.664 (0.000)	1.394 (0.057)	1.231 (0.051)	2.324 (0.139)	1.388 (0.071)	1.226 (0.063)	2.221 (0.185)	
TimesNet	1.143 (0.000)	1.009 (0.000)	1.590 (0.000)	1.378 (0.054)	1.217 (0.048)	2.271 (0.128)	1.378 (0.068)	1.217 (0.060)	2.193 (0.174)	
MICN	1.170 (0.000)	1.033 (0.000)	1.688 (0.000)	1.400 (0.058)	1.236 (0.051)	2.345 (0.142)	1.395 (0.071)	1.232 (0.063)	2.243 (0.188)	
SCINet	1.166 (0.000)	1.030 (0.000)	1.660 (0.000)	1.404 (0.056)	1.240 (0.050)	2.355 (0.136)	1.392 (0.074)	1.230 (0.065)	2.237 (0.192)	
StemGNN	1.166 (0.000)	1.030 (0.000)	1.671 (0.000)	1.401 (0.057)	1.237 (0.050)	2.345 (0.139)	1.394 (0.073)	1.231 (0.064)	2.239 (0.190)	
FreTS	1.168 (0.000)	1.031 (0.000)	1.663 (0.000)	1.407 (0.056)	1.242 (0.049)	2.362 (0.136)	1.396 (0.073)	1.233 (0.065)	2.247 (0.191)	
Koopa	1.193 (0.000)	1.053 (0.000)	1.716 (0.000)	1.394 (0.057)	1.231 (0.051)	2.325 (0.139)	1.395 (0.073)	1.232 (0.065)	2.244 (0.191)	
DLInear	1.159 (0.000)	1.024 (0.000)	1.651 (0.000)	1.405 (0.056)	1.240 (0.049)	2.357 (0.136)	1.394 (0.072)	1.231 (0.063)	2.240 (0.186)	
FiLM	1.208 (0.000)	1.067 (0.000)	1.784 (0.000)	1.398 (0.058)	1.235 (0.051)	2.340 (0.140)	1.399 (0.076)	1.236 (0.067)	2.260 (0.200)	
CSDI	1.178 (0.000)	1.040 (0.000)	1.696 (0.000)	1.401 (0.057)	1.237 (0.050)	2.345 (0.138)	1.394 (0.074)	1.231 (0.066)	2.241 (0.196)	
US-GAN	1.163 (0.000)	1.027 (0.000)	1.637 (0.000)	1.399 (0.058)	1.235 (0.051)	2.341 (0.141)	1.389 (0.080)	1.227 (0.071)	2.228 (0.213)	
GP-VAE	1.159 (0.000)	1.024 (0.000)	1.652 (0.000)	1.403 (0.059)	1.239 (0.052)	2.355 (0.145)	1.397 (0.073)	1.234 (0.064)	2.249 (0.192)	
Mean	1.209 (0.000)	1.067 (0.000)	1.716 (0.000)	1.424 (0.069)	1.258 (0.061)	2.416 (0.178)	1.445 (0.075)	1.276 (0.067)	2.390 (0.213)	
Median	1.208 (0.001)	1.066 (0.001)	1.717 (0.001)	1.423 (0.069)	1.257 (0.061)	2.415 (0.176)	1.448 (0.072)	1.278 (0.063)	2.398 (0.202)	
LOCF	1.194 (0.020)	1.054 (0.017)	1.682 (0.050)	1.417 (0.066)	1.251 (0.058)	2.395 (0.168)	1.430 (0.076)	1.263 (0.067)	2.346 (0.212)	
Linear	1.188 (0.020)	1.049 (0.018)	1.677 (0.044)	1.414 (0.064)	1.248 (0.057)	2.385 (0.162)	1.422 (0.077)	1.256 (0.068)	2.321 (0.212)	

	ETT_h1 (point_50%)								
	MAE w/ XGB	MRE w/ XGB	MSE w/ XGB	MAE w/ RNN	MRE w/ RNN	MSE w/ RNN	MAE w/ Transformer	MRE w/ Transformer	MSE w/ Transformer
Transformer	1.224 (0.000)	1.081 (0.000)	1.778 (0.000)	1.377 (0.062)	1.216 (0.055)	2.280 (0.151)	1.406 (0.069)	1.242 (0.061)	2.285 (0.185)
SAlTS	1.175 (0.000)	1.038 (0.000)	1.654 (0.000)	1.402 (0.056)	1.238 (0.050)	2.349 (0.136)	1.401 (0.083)	1.237 (0.074)	2.262 (0.224)
Nonstationary	1.227 (0.000)	1.083 (0.000)	1.802 (0.000)	1.446 (0.061)	1.276 (0.054)	2.484 (0.154)	1.384 (0.087)	1.222 (0.076)	2.236 (0.202)
ETStformer	1.222 (0.000)	1.079 (0.000)	1.885 (0.000)	1.329 (0.060)	1.173 (0.053)	2.125 (0.138)	1.351 (0.061)	1.193 (0.054)	2.113 (0.153)
PatchTST	1.234 (0.000)	1.090 (0.000)	1.840 (0.000)	1.398 (0.059)	1.235 (0.052)	2.344 (0.143)	1.370 (0.074)	1.210 (0.066)	2.176 (0.192)
Crossformer	1.228 (0.000)	1.084 (0.000)	1.838 (0.000)	1.391 (0.058)	1.228 (0.051)	2.323 (0.141)	1.380 (0.070)	1.218 (0.062)	2.204 (0.181)
Informor	1.214 (0.000)	1.072 (0.000)	1.782 (0.000)	1.391 (0.059)	1.229 (0.052)	2.315 (0.142)	1.398 (0.076)	1.234 (0.068)	2.252 (0.205)
Autoformer	1.348 (0.000)	1.190 (0.000)	2.060 (0.000)	1.450 (0.108)	1.280 (0.095)	2.444 (0.368)	1.442 (0.155)	1.273 (0.137)	2.438 (0.520)
Pyraformer	1.169 (0.000)	1.032 (0.000)	1.640 (0.000)	1.366 (0.057)	1.206 (0.050)	2.235 (0.134)	1.373 (0.071)	1.212 (0.063)	2.176 (0.186)
Transformer	1.170 (0.000)	1.034 (0.000)	1.631 (0.000)	1.378 (0.056)	1.217 (0.049)	2.275 (0.133)	1.357 (0.081)	1.198 (0.072)	2.130 (0.213)
BRITS	1.177 (0.000)	1.039 (0.000)	1.680 (0.000)	1.371 (0.061)	1.210 (0.054)	2.259 (0.147)	1.364 (0.076)	1.205 (0.068)	2.155 (0.198)
MRNN	1.070 (0.000)	0.945 (0.000)	1.417 (0.000)	1.250 (0.076)	1.104 (0.067)	1.900 (0.190)	1.379 (0.088)	1.218 (0.051)	2.216 (0.142)
GRU4Rec	1.205 (0.000)	1.064 (0.000)	1.870 (0.000)	1.339 (0.061)	1.182 (0.054)	2.154 (0.145)	1.326 (0.074)	1.171 (0.065)	2.043 (0.192)
TimesNet	1.127 (0.000)	0.995 (0.000)	1.513 (0.000)	1.333 (0.054)	1.177 (0.048)	2.149 (0.125)	1.316 (0.066)	1.162 (0.058)	2.027 (0.163)
MICN	1.163 (0.000)	1.027 (0.000)	1.611 (0.000)	1.305 (0.078)	1.152 (0.069)	2.049 (0.189)	1.379 (0.070)	1.218 (0.062)	2.185 (0.195)
SCINet	1.174 (0.000)	1.037 (0.000)	1.654 (0.000)	1.411 (0.055)	1.246 (0.049)	2.390 (0.134)	1.375 (0.080)	1.214 (0.070)	2.203 (0.209)
StemGNN	1.139 (0.000)	1.006 (0.000)	1.561 (0.000)	1.392 (0.057)	1.229 (0.051)	2.311 (0.139)	1.410 (0.078)	1.245 (0.069)	2.285 (0.212)
FreTS	1.207 (0.000)	1.066 (0.000)	1.764 (0.000)	1.406 (0.056)	1.242 (0.050)	2.361 (0.136)	1.397 (0.082)	1.233 (0.073)	2.252 (0.219)
Koopa	1.227 (0.000)	1.084 (0.000)	1.804 (0.000)	1.384 (0.064)	1.222 (0.056)	2.304 (0.153)	1.419 (0.086)	1.253 (0.055)	2.315 (0.169)
DLInear	1.216 (0.000)	1.074 (0.000)	1.808 (0.000)	1.380 (0.056)	1.219 (0.049)	2.283 (0.132)	1.397 (0.067)	1.234 (0.067)	2.254 (0.200)
FiLM	1.247 (0.000)	1.101 (0.000)	1.880 (0.000)	1.379 (0.057)	1.218 (0.051)	2.281 (0.137)	1.442 (0.048)	1.273 (0.042)	2.391 (0.134)
CSDI	1.136 (0.000)	1.003 (0.000)	1.550 (0.000)	1.373 (0.050)	1.212 (0.044)	2.256 (0.144)	1.393 (0.070)	1.230 (0.062)	2.245 (0.184)
US-GAN	1.155 (0.000)	1.019 (0.000)	1.691 (0.000)	1.299 (0.040)	1.147 (0.036)	2.022 (0.103)	1.283 (0.055)	1.133 (0.048)	1.944 (0.144)
GP-VAE	1.178 (0.000)	1.040 (0.000)	1.721 (0.000)	1.336 (0.066)	1.180 (0.058)	2.179 (0.156)	1.340 (0.076)	1.183 (0.068)	2.098 (0.203)
Mean	1.431 (0.000)	1.264 (0.000)	2.304 (0.000)	1.512 (0.120)	1.335 (0.106)	2.625 (0.351)	1.627 (0.072)	1.437 (0.064)	3.010 (0.233)
Median	1.517 (0.086)	1.340 (0.076)	2.572 (0.269)	1.531 (0.128)	1.352 (0.113)	2.705 (0.382)	1.671 (0.069)	1.476 (0.061)	3.142 (0.213)
LOCF	1.446 (0.123)	1.277 (0.109)	2.416 (0.312)	1.477 (0.134)	1.304 (0.118)	2.552 (0.388)	1.571 (0.158)	1.388 (0.139)	2.821 (0.501)
Linear	1.393 (0.140)	1.230 (0.124)	2.281 (0.357)	1.453 (0.127)	1.283 (0.112)	2.486 (0.362)	1.525 (0.163)	1.347 (0.144)	2.670 (0.516)

Table 21: Performance comparison for the forecasting task on ETT_h1 datasets with 10% point missing and 50% point missing.

ETT_h1 (point_10%)												
	MAE	wt XGB	MRE	wt XGB	MAE	wt XGB	MRE	wt XGB	MAE	wt XGB	MRE	wt XGB
Transformer	MAE	wt XGB	MRE	wt XGB	MAE	wt XGB	MRE	wt XGB	MAE	wt XGB	MRE	wt XGB
Transformer	1.114 (0.000)	0.985 (0.000)	1.453 (0.000)	1.266 (0.065)	1.119 (0.057)	2.002 (0.132)	0.376 (0.343)	0.332 (0.303)	0.305 (0.478)			
SATS	1.146 (0.000)	1.014 (0.000)	1.503 (0.000)	1.268 (0.065)	1.121 (0.057)	2.012 (0.131)	0.399 (0.332)	0.352 (0.294)	0.317 (0.469)			
Nonstationary	1.137 (0.000)	1.006 (0.000)	1.508 (0.000)	1.287 (0.063)	1.138 (0.056)	2.059 (0.127)	0.383 (0.348)	0.339 (0.308)	0.315 (0.490)			
ETSTransformer	1.117 (0.000)	0.988 (0.000)	1.459 (0.000)	1.266 (0.063)	1.120 (0.056)	2.002 (0.128)	0.398 (0.332)	0.352 (0.294)	0.317 (0.468)			
PatchTS	1.151 (0.000)	1.018 (0.000)	1.558 (0.000)	1.272 (0.062)	1.125 (0.055)	2.022 (0.125)	0.385 (0.337)	0.340 (0.298)	0.309 (0.473)			
Crossformer	1.130 (0.000)	0.999 (0.000)	1.494 (0.000)	1.270 (0.063)	1.119 (0.056)	2.016 (0.127)	0.390 (0.335)	0.345 (0.296)	0.312 (0.470)			
Informr	1.089 (0.000)	0.963 (0.000)	1.396 (0.000)	1.267 (0.064)	1.121 (0.057)	2.008 (0.129)	0.386 (0.341)	0.342 (0.301)	0.312 (0.474)			
Autoformer	1.121 (0.000)	0.991 (0.000)	1.467 (0.000)	1.270 (0.063)	1.123 (0.055)	2.014 (0.125)	0.395 (0.334)	0.349 (0.295)	0.318 (0.470)			
Pyrformer	1.104 (0.000)	0.977 (0.000)	1.439 (0.000)	1.271 (0.062)	1.124 (0.055)	2.018 (0.126)	0.390 (0.338)	0.345 (0.299)	0.314 (0.474)			
Transformer	1.092 (0.000)	0.966 (0.000)	1.368 (0.000)	1.268 (0.063)	1.121 (0.056)	2.009 (0.127)	0.397 (0.334)	0.351 (0.295)	0.318 (0.469)			
BRITS	1.063 (0.000)	0.940 (0.000)	1.299 (0.000)	1.266 (0.064)	1.119 (0.056)	2.008 (0.129)	0.406 (0.329)	0.359 (0.291)	0.322 (0.466)			
MRNN	1.051 (0.000)	0.950 (0.000)	1.279 (0.000)	1.228 (0.071)	1.086 (0.063)	1.894 (0.146)	0.394 (0.334)	0.348 (0.295)	0.312 (0.473)			
GRU	1.131 (0.000)	1.001 (0.000)	1.467 (0.000)	1.260 (0.064)	1.114 (0.056)	1.983 (0.130)	0.388 (0.339)	0.344 (0.300)	0.312 (0.475)			
TimesNet	1.111 (0.000)	0.983 (0.000)	1.425 (0.000)	1.250 (0.063)	1.105 (0.056)	1.956 (0.125)	0.396 (0.334)	0.350 (0.295)	0.317 (0.472)			
MICN	1.131 (0.000)	1.000 (0.000)	1.509 (0.000)	1.266 (0.065)	1.120 (0.057)	2.000 (0.132)	0.400 (0.329)	0.353 (0.294)	0.318 (0.472)			
SCINet	1.139 (0.000)	1.007 (0.000)	1.513 (0.000)	1.269 (0.063)	1.123 (0.056)	2.016 (0.127)	0.387 (0.335)	0.342 (0.297)	0.310 (0.471)			
StemGNN	1.122 (0.000)	0.992 (0.000)	1.507 (0.000)	1.269 (0.064)	1.122 (0.056)	2.013 (0.129)	0.394 (0.332)	0.349 (0.294)	0.314 (0.470)			
FreTS	1.135 (0.000)	1.004 (0.000)	1.507 (0.000)	1.274 (0.063)	1.127 (0.055)	2.030 (0.127)	0.385 (0.338)	0.341 (0.299)	0.310 (0.474)			
Koopa	1.165 (0.000)	1.030 (0.000)	1.581 (0.000)	1.263 (0.064)	1.117 (0.057)	1.991 (0.129)	0.376 (0.344)	0.333 (0.304)	0.306 (0.479)			
DLInear	1.135 (0.000)	1.004 (0.000)	1.504 (0.000)	1.272 (0.062)	1.125 (0.055)	2.021 (0.126)	0.394 (0.293)	0.348 (0.293)	0.313 (0.468)			
FILM	1.147 (0.000)	1.014 (0.000)	1.589 (0.000)	1.269 (0.061)	1.122 (0.054)	2.009 (0.122)	0.387 (0.335)	0.342 (0.314)	0.321 (0.507)			
CSDI	1.085 (0.000)	0.960 (0.000)	1.356 (0.000)	1.266 (0.064)	1.120 (0.056)	2.009 (0.129)	0.398 (0.331)	0.352 (0.293)	0.317 (0.466)			
US-GAN	1.086 (0.000)	0.960 (0.000)	1.363 (0.000)	1.272 (0.062)	1.125 (0.055)	2.026 (0.127)	0.418 (0.329)	0.370 (0.291)	0.336 (0.471)			
GP-VAE	1.146 (0.000)	1.013 (0.000)	1.522 (0.000)	1.264 (0.066)	1.118 (0.058)	1.999 (0.134)	0.386 (0.342)	0.341 (0.303)	0.312 (0.484)			
Mean	1.112 (0.000)	0.984 (0.000)	1.423 (0.000)	1.271 (0.070)	1.125 (0.062)	2.013 (0.148)	0.420 (0.329)	0.371 (0.291)	0.330 (0.484)			
Median	1.114 (0.002)	0.986 (0.002)	1.434 (0.011)	1.273 (0.072)	1.126 (0.064)	2.018 (0.153)	0.411 (0.333)	0.363 (0.295)	0.325 (0.485)			
LOCF	1.118 (0.005)	0.989 (0.005)	1.432 (0.026)	1.271 (0.070)	1.124 (0.062)	2.013 (0.147)	0.404 (0.336)	0.357 (0.297)	0.322 (0.483)			
Linear	1.124 (0.012)	0.995 (0.011)	1.466 (0.033)	1.270 (0.069)	1.124 (0.061)	2.013 (0.143)	0.404 (0.335)	0.357 (0.296)	0.323 (0.480)			

ETT_h1 (point_50%)												
	MAE	wt XGB	MRE	wt XGB	MAE	wt XGB	MRE	wt XGB	MAE	wt XGB	MRE	wt XGB
Transformer	MAE	wt XGB	MRE	wt XGB	MAE	wt XGB	MRE	wt XGB	MAE	wt XGB	MRE	wt XGB
Transformer	1.223 (0.000)	1.082 (0.000)	1.683 (0.000)	1.240 (0.071)	1.096 (0.062)	1.937 (0.145)	0.379 (0.337)	0.335 (0.298)	0.303 (0.476)			
SATS	1.156 (0.000)	1.023 (0.000)	1.616 (0.000)	1.274 (0.062)	1.126 (0.055)	2.022 (0.127)	0.375 (0.341)	0.332 (0.301)	0.306 (0.474)			
Nonstationary	1.196 (0.000)	1.066 (0.000)	1.657 (0.000)	1.317 (0.065)	1.164 (0.057)	2.119 (0.134)	0.378 (0.369)	0.334 (0.326)	0.323 (0.530)			
ETSTransformer	1.205 (0.000)	1.066 (0.000)	1.835 (0.000)	1.235 (0.061)	1.092 (0.054)	1.881 (0.116)	0.321 (0.343)	0.284 (0.303)	0.259 (0.449)			
PatchTS	1.192 (0.000)	1.054 (0.000)	1.687 (0.000)	1.264 (0.058)	1.118 (0.051)	2.002 (0.113)	0.370 (0.331)	0.327 (0.292)	0.292 (0.454)			
Crossformer	1.180 (0.000)	1.044 (0.000)	1.651 (0.000)	1.268 (0.062)	1.122 (0.055)	2.007 (0.126)	0.377 (0.324)	0.334 (0.287)	0.294 (0.449)			
Informr	1.128 (0.000)	0.998 (0.000)	1.502 (0.000)	1.269 (0.059)	1.122 (0.052)	1.990 (0.118)	0.384 (0.347)	0.340 (0.307)	0.314 (0.490)			
Autoformer	1.306 (0.000)	1.155 (0.000)	1.948 (0.000)	1.287 (0.177)	1.138 (0.157)	2.069 (0.454)	0.559 (0.102)	0.494 (0.090)	0.402 (0.129)			
Pyrformer	1.120 (0.000)	0.990 (0.000)	1.442 (0.000)	1.247 (0.055)	1.103 (0.049)	1.919 (0.106)	0.374 (0.337)	0.331 (0.298)	0.297 (0.469)			
Transformer	1.177 (0.000)	1.041 (0.000)	1.634 (0.000)	1.243 (0.057)	1.100 (0.051)	1.923 (0.110)	0.375 (0.334)	0.332 (0.295)	0.297 (0.464)			
BRITS	1.220 (0.000)	1.079 (0.000)	1.764 (0.000)	1.254 (0.059)	1.109 (0.052)	1.961 (0.117)	0.399 (0.332)	0.353 (0.293)	0.319 (0.473)			
MRNN	0.984 (0.000)	0.870 (0.000)	1.179 (0.000)	1.081 (0.089)	0.956 (0.079)	1.497 (0.175)	0.445 (0.296)	0.394 (0.261)	0.337 (0.347)			
GRU	1.210 (0.000)	1.070 (0.000)	1.828 (0.000)	1.215 (0.057)	1.075 (0.051)	1.810 (0.115)	0.359 (0.340)	0.318 (0.301)	0.286 (0.461)			
TimesNet	1.143 (0.000)	1.011 (0.000)	1.486 (0.000)	1.202 (0.063)	1.063 (0.056)	1.806 (0.119)	0.365 (0.329)	0.323 (0.291)	0.290 (0.447)			
MICN	1.130 (0.000)	0.999 (0.000)	1.495 (0.000)	1.178 (0.081)	1.042 (0.072)	1.716 (0.163)	0.343 (0.355)	0.304 (0.315)	0.283 (0.477)			
SCINet	1.095 (0.000)	0.968 (0.000)	1.407 (0.000)	1.254 (0.063)	1.109 (0.056)	1.975 (0.125)	0.372 (0.339)	0.329 (0.299)	0.300 (0.473)			
StemGNN	1.113 (0.000)	0.985 (0.000)	1.437 (0.000)	1.259 (0.057)	1.113 (0.050)	1.967 (0.115)	0.362 (0.346)	0.320 (0.306)	0.294 (0.477)			
FreTS	1.173 (0.000)	1.038 (0.000)	1.587 (0.000)	1.259 (0.059)	1.114 (0.052)	1.984 (0.118)	0.367 (0.336)	0.325 (0.297)	0.293 (0.463)			
Koopa	1.288 (0.000)	1.139 (0.000)	1.855 (0.000)	1.265 (0.068)	1.119 (0.060)	1.973 (0.138)	0.357 (0.356)	0.316 (0.315)	0.297 (0.494)			
DLInear	1.176 (0.000)	1.040 (0.000)	1.616 (0.000)	1.262 (0.054)	1.116 (0.048)	1.981 (0.101)	0.368 (0.336)	0.326 (0.297)	0.295 (0.466)			
FILM	1.215 (0.000)	1.075 (0.000)	1.686 (0.000)	1.283 (0.062)	1.135 (0.055)	2.054 (0.129)	0.376 (0.376)	0.333 (0.332)	0.319 (0.537)			
CSDI	1.183 (0.000)	1.047 (0.000)	1.641 (0.000)	1.269 (0.063)	1.122 (0.055)	1.995 (0.134)	0.362 (0.337)	0.321 (0.298)	0.290 (0.459)			
US-GAN	1.083 (0.000)	0.958 (0.000)	1.414 (0.000)	1.114 (0.076)	0.985 (0.067)	1.603 (0.172)	0.352 (0.267)	0.311 (0.236)	0.240 (0.336)			
GP-VAE	1.170 (0.000)	1.035 (0.000)	1.643 (0.000)	1.169 (0.071)	1.034 (0.063)	1.738 (0.139)	0.344 (0.349)	0.304 (0.309)	0.282 (0.468)			
Mean	1.472 (0.000)	1.302 (0.000)	2.410 (0.000)	1.368 (0.147)	1.210 (0.130)	2.237 (0.368)	0.677 (0.346)	0.599 (0.306)	0.645 (0.481)			
Median	1.498 (0.026)	1.325 (0.023)	2.493 (0.083)	1.380 (0.147)	1.221 (0.130)	2.281 (0.372)	0.588 (0.404)	0.520 (0.357)	0.563 (0.523)			
LOCF	1.411 (0.126)	1.248 (0.112)	2.270 (0.323)	1.327 (0.146)	1.174 (0.129)	2.143 (0.368)	0.523 (0.392)	0.463 (0.347)	0.480 (0.519)			
Linear	1.356 (0.144)	1.200 (0.127)	2.118 (0.384)	1.306 (0.136)	1.155 (0.120)	2.093 (0.337)	0.492 (0.382)	0.435 (0.338)	0.440 (0.514)			

